

**THERMODYNAMIC PARAMETERS AND
ADSORPTION KINETICS OF ORGANIC
COMPOUNDS FORMING THE COMPACT
ADSORPTION LAYER AT BI SINGLE
CRYSTAL ELECTRODES**

HEILI KASUK



TARTU UNIVERSITY
PRESS

Department of Chemistry, Institute of Physical Chemistry, Chair of Physical Chemistry, University of Tartu, Estonia

Dissertation of physical and electrochemistry

Dissertation is accepted for the commencement of the degree of Doctor of Philosophy in Chemistry on June 29, 2007, by the Doctoral Committee of the Department of Chemistry, University of Tartu.

Doctoral advisors: Prof. Enn Lust, University of Tartu
Ph. D. Gunnar Nurk, University of Tartu

Opponents: Prof. Renat R. Nazmutdinov (Kazan State Technological University, 420015 Kazan, Republic Tatarstan, Russia)

Prof. Emer. Vello Past (University of Tartu, Estonia)

Commencement: 11⁰⁰ August 30 2007, in Tartu, 18 Ülikooli Str., in the University council hall

ISSN 1406–7366

ISBN 978–9949–11–664–5 (trükis)

ISBN 978–9949–11–665–2 (PDF)

Autoriõigus Heili Kasuk, 2007

Tartu Ülikooli Kirjastus

www.tyk.ee

Tellimus nr. 299

to my parents

TABLE OF CONTENTS

1. LIST OF ORIGINAL PUBLICATIONS	9
2. ABBREVIATIONS AND SYMBOLS	10
3. INTRODUCTION	13
4. LITERATURE OVERVIEW.....	15
4.1. Thermodynamic conceptions of adsorption and basic equations for the calculation of the adsorption parameters of organic compounds at metal electrodes	15
4.2. Adsorption kinetics of organic compounds.....	18
4.3. Phase transition in two-dimensional adlayers at electrode surface: thermodynamics, kinetics and structural aspects.....	22
4.4. Fitting of impedance data of two-dimensional adlayers.....	26
5. EXPERIMENTAL.....	30
6. RESULTS AND DISCUSSIONS.....	31
6.1. Adsorption of uracil on bismuth single crystal planes [I, III]	31
6.1.1. Simulation of impedance data	33
6.1.2. Estimation of limiting stages [I]	34
6.1.3. Adsorption isotherms and thermodynamic adsorption parameters [III]	36
6.2. Adsorption of sodium dodecyl sulfate on bismuth single crystal planes [VI].....	39
6.2.1. Calculation of the complex impedance plane plot parameters	41
6.2.2. Estimation of the limiting stage using classical analysis model	42
6.2.3. Thermodynamic adsorption parameters [VI].....	43
6.3. Adsorption of camphor and 2, 2'-bipyridine on Bi(111)electrode surface [IV, V].....	45
6.4. Comparison of some adsorption kinetic and thermodynamic parameters of uracil, tetrabutylammonium cations, sodium dodecyl sulfate, camphor and 2, 2'-bipyridin on Bi single crystal plane.....	48
6.4.1. Analysis of Nyquist plots	48
6.4.2. Estimation of the limiting stage.....	49
6.4.3. Thermodynamic adsorption parameters	51
7. SUMMARY.....	53
8. REFERENCES	55

9. SUMMARY IN ESTONIAN.....	59
10. ACKNOWLEDGEMENT	61
11. PUBLICATIONS.....	63

1. LIST OF ORIGINAL PUBLICATIONS

- I H. Kasuk**, G. Nurk, K. Lust and E. Lust, Adsorption kinetics of uracil on the bismuth single crystal planes, *J. Electroanal. Chem.* 550–551 (2003) 13–31.
Author's contribution: performing all kinetic measurements, modelling and interpretations.
- II K. Laes, H. Kasuk**, G. Nurk, M. Väärtnõu, K. Lust, A. Jänes and E. Lust, Adsorption kinetics of tetrabutylammonium cations on Bi(01 $\bar{1}$) plane, *J. of Electroanal. Chem.*, 569 (2004) 241–256.
Author's contribution: participated in kinetic measurements, calculations and modelling, and writing the paper.
- III H. Kasuk**, G. Nurk, K. Lust and E. Lust, Adsorption of uracil on bismuth single crystal planes, *J. Electroanal. Chem.*, 580 (2005) 128–134.
Author's contribution: performing all measurements, modelling, interpretations and writing the paper.
- IV S. Kallip, H. Kasuk**, V. Grozovski, E. Lust, Adsorption of camphor at Bi(111) electrode, *ECS Transactions*, 3 (2007), accepted.
Author's contribution: performing all kinetic measurements, modelling and participated writing the paper.
- V S. Kallip, H. Kasuk**, V. Grozovski, P. Möller, E. Lust, Adsorption kinetics of camphor and 2, 2'-bipyridin on Bi(111) electrode surface, *Electrochim. Acta*, in review.
Author's contribution: performing all kinetic measurements, modelling and participated writing the paper
- VI H. Kasuk**, G. Nurk, E. Lust, Adsorption of dodecyl sulfate anions on the bismuth (111), (001) and (01 $\bar{1}$) planes, *J. Electroanal. Chem.*, in press.
Author's contribution: participated in calculations and modelling and writing the paper.

2. ABBREVIATIONS AND SYMBOLS

a	attraction interaction constant in the Frumkin adsorption isotherm
a_i	activity of chemical component i
a_{org}	activity of organic compound in the solution
ac	alternating current
B	adsorption equilibrium constant in the Frumkin adsorption isotherm
B_{max}	adsorption equilibrium constant at the maximal adsorption potential $E=E_{max}$
c	total concentration of solution
C	differential capacitance
C^*	limiting differential capacitance, when surface coverage $\theta=1$
C_0	thermodynamic equilibrium differential capacitance, when $\theta=0$ and ac frequency $f \rightarrow 0$
C_{ad}	adsorption capacitance
c_{cat}	adsorbate concentration
C_n	differential ‘needle peek’ capacitance
C_{true}	differential capacitance as ac frequency $f \rightarrow \infty$
C_p	parallel interfacial differential capacitance
C_s	series differential capacitance
C_{sat}	saturation capacitance
CH	cyclohexanol
CPE	constant phase element
D	effective diffusion coefficient
E	electrode potential
E_{max}	maximal adsorption potential
E_N	limiting adsorption potential shift of zero charge potential, $\theta=1$
$E_{\sigma=0}$	zero charge potential
EDL	electrical double layer
EDLC	electrical double layer capacitor
f	ac frequency
FMG	Frumkin-Melik-Gaikazyan model
FMGC ₁	modified Frumkin-Melik-Gaikazyan model
HF	high frequency maximum
j	imaginary unit, $j=\sqrt{-1}$
j	current density
$k_{ad}, k_a,$	adsorption and desorption rate constants, respectively
$k_g, k_d, k_d, k_g,$	rate constant of the cluster growth and dissolution process constants, respectively
$k_1; k_2; k_3$	constants characterizing the process of two-dimensional association of organic molecules
LB	Langmuir-Blodgett films
LTSE	low-temperature series expansion model

MBE	molecular beam epitaxy
MFA	Frumkin adsorption model
<i>n</i> -HepOH	<i>n</i> -Heptanol or 1-Heptanol
N_A	Avogadro's number
p	pressure
QCA	quasi-chemical approximation
R	gas constant
R_{ct}	charge transfer resistance
R_{el}	base electrolyte resistance
R_D	diffusion resistance
R_n	'needle peak' resistance
R_p	parallel resistance
R_s	series resistance
S	area of cluster
S_A	area engaged by one adsorbed molecule
SAM	self-assembled monolayer
SDS	sodium dodecyl sulfate
SEIRAS	time-resolved infrared spectroscopy
t	time
T	absolute temperature
TBA ⁺	tetrabutylammonium cation
<i>tert</i> -PenOH	<i>tert</i> -pentanol or 2-methyl-2-butanol
x	distance from the plane of adsorption at the electrode
$Z_{A-A}, Z_{W-A}, Z_{W-W}$	particle-particle interaction energy, where W stands for water and A for adsorbate
Z_w	Warburg-like diffusion impedance
α	fractional exponent
β, β', β''	depression angles calculated from Cole-Cole plots
χ^2	chi-square function
γ	interfacial tension
γ'	reversible surface work
Γ_i	Gibbs adsorption of component i
Γ_{max}	maximal Gibbs adsorption of adsorbate
Γ_{org}	Gibbs adsorption of neutral organic compound
Δ^2	weighted sum of the squares
ΔG_{ads}^0	standard Gibbs energy of adsorption
ΔG_{int}^0	standard Gibbs energy of intermolecular interaction
ε_{AA}	nearest-neighbor interaction energy
ε'	real part of the complex dielectric constant
ε''	imaginary part of the complex dielectric constant
ε^*	complex dielectric constant
μ	chemical potential
μ_i	chemical potential of the component i

v	net rate of adsorption due to the departure from equilibrium conditions
v_0	adsorption exchange rate
π	surface pressure of the adsorbate
θ	surface coverage
θ_{max}	maximal surface coverage
σ	surface charge density
σ'	surface charge density when surface coverage $\theta=1$
σ_0	surface charge density of the base electrolyte
σ_1	surface charge density of the area covered by clusters
τ_D^{theor}	diffusion (theoretical) controlled relaxation time constants
τ_K^{theor}	theoretical relaxation time constant of heterogeneous charge transfer process
τ_{exp}	experimental relaxation time constant, calculated from $(\omega R_p)^{-1}$, C_p -dependence
τ_{exp}^*	experimental relaxation time constant obtained by Eq.6.1.2.1
τ_m	experimental relaxation frequency obtained from Nyquist plots
ω	angular frequency (equal to $2\pi f$)
ω_0	exchange rate of molecules in the condition of two dimensional associations
ω_m	experimental angular frequency obtained from Nyquist plots
(hkl)	the notation of the Bi crystallographic plane (index)
2D	two-dimensional
2, 2'-BP	2, 2'-bipyridin
3D	three dimensional

3. INTRODUCTION

Adsorption of organic compounds at the metal|electrolyte solution interface is attracting considerable attention of everyone concerning with theoretical and applied electrochemistry. Indeed, unless the adsorption effects are taken into account it is impossible to understand the mechanism of most of the processes occurring at the mercury and solid electrode surface and therefore to interpret the results of electrochemical kinetics.

Adsorption of organic compounds is widely used for regulating the processes of metal electrodeposition. Adsorption as well as desorption determines the behaviour of organic compounds at positive electrodes of fuel cells and therefore their suitability as electrochemical fuel. The action of corrosion inhibitors is based on adsorption effects and they must also be taken into consideration in investigations for new routes of organic electrochemical synthesis. Adsorption effects are also met in the general electrochemical industry. Investigations of adsorption phenomena at electrode|solution interfaces are of noticeable theoretical interest, extending our knowledge about the structure of the electrical double layer.

Adsorption and desorption are very complicated processes at solid electrodes because the crystallographic structure has very noticeable effect on the thermodynamic adsorption parameters as well as adsorption kinetics. Solid electrodes are usually geometrically inhomogeneous and this aspect causes the formation of the non-homogeneous adsorption layer structure at real solid surfaces. Therefore the thermodynamic and kinetic studies of adsorption at single crystal plane electrodes can be taken as only a first step forward development of the molecular level adsorption theory at energetically homogeneous as well as non-homogeneous polycrystalline surfaces.

It was demonstrated using *in situ* STM method that the electrode potential, surface charge density and nature of the base electrolyte ions has noticeable effect on the molecular structure of adsorption layer for camphor + Na₂SO₄ | Bi(111) interface. The weak specific adsorption of SO₄²⁻ anions at positively charged Bi(111) surface indicates the camphor compact adsorption layer formation at Bi(111). However compounds demonstrating only the physical adsorption nature (1-hexanol, 1-heptanol, dodecyl sulfate anions) are unable to form very compact adsorption layers at Bi(111) electrode interface, very well detectable using *in situ* STM method.

Adsorption/desorption kinetics thus charge accumulation and release kinetics is extremely important for the development of the electrochemically efficient electrical double layer capacitors (EDLC), because the peak power density of EDLC is primarily related with the rate of desorption of organic cations and anions adsorbed at electrodes. However taking into account the process nature at the nanoporous EDLC electrodes at first the adsorption mechanism of tetraalkylammonium cation and dodecyl sulfate anions at single

crystal plane electrodes is extremely important, because in addition to the slow heterogeneous adsorption step the mass transfer limitations can complicate the kinetic analysis of adsorption at nanoporous electrodes.

Uracil, sodium dodecyl sulfate, tetrabutylammonium cation, camphor and 2, 2'-bipyridin were chosen because (1) adsorption of these compounds has been well investigated on Hg, Ag and Au planes; (2) they are forming compact adsorption layers; and (3) can be investigated in a wide potential region.

The main aim of this work was to establish the nature of the limiting stages and to obtain the kinetic and thermodynamic parameters of uracil, SDS, camphor, TBA⁺ and 2,2'-BP adsorption on the various Bi planes within the wide range of concentrations and electrode potentials.

4. LITERATURE OVERVIEW

4.1. Thermodynamic conceptions of adsorption and basic equations for the calculation of the adsorption parameters of organic compounds at metal electrodes

The thermodynamic method for the calculation of the adsorption parameters of organic compound on metal electrode is based on the fundamental electrocapillary equation and at constant pressure and temperature it can be written in the form [1, 7]

$$d\gamma = -\sigma dE - \sum \Gamma_i d\mu_i = -\sigma dE - RT \sum \Gamma_i d \ln a_i \quad (4.1.1)$$

where γ and σ are the interfacial tension and surface charge density respectively; Γ_i , a_i and μ_i are Gibbs adsorption, activity and chemical potential of the component i , respectively, T is the absolute temperature and R is the gas constant. If $a_i = \text{const.}$, then $d \ln a_i = 0$, and under these circumstances the so-called Lippmann equation can be received

$$-\sigma = \left(\frac{\partial \gamma}{\partial E} \right)_{a_i} \quad (4.1.2)$$

According to the Lippmann equation the differential capacitance is obtained as

$$C = \frac{d\sigma}{dE} \quad (4.1.3)$$

and after substitution of Eq. (4.1.3) into the Eq. (4.1.2) we can get the relationship for the differential capacitance

$$C = \frac{d\sigma}{dE} = - \left(\frac{\partial^2 \gamma}{\partial E^2} \right)_{a_i} \quad (4.1.4)$$

For solid electrodes, to a first approximation, the interfacial tension γ should be replaced by the reversible surface work γ' term [1,6,7] in Eq. (4.1.4).

According to the Eq. (4.1.1) the Gibbs adsorption of neutral organic compound on the electrode surface at constant potential, temperature and pressure is defined by

$$\Gamma_{org} = -\frac{1}{RT} \left(\frac{\partial \gamma'}{\partial \ln a_{org}} \right)_{E,T,p} \quad (4.1.5)$$

where a_{org} is the activity of organic compound in the solution [6].

Nonthermodynamic methods for the calculation of the adsorption parameters of organic compounds at the metal electrodes are based on various electrical double layer (EDL) models and physical conceptions [1,7,8,14,23].

The first quantitative theory for adsorption of organic compounds at liquid electrodes has been developed by A. N. Frumkin at 1925 [18] and nowadays the various modern models are based on this model. In this conception the behaviour of organic compound at metal electrode is discussed as the two parallel capacitor equivalent circuit, where one of the capacitor characterize the adsorbed electrolyte on the electrode surface and the other characterize capacitor are determined by the adsorbed organic compound monolayer parameters. The surface charge for such a system is defined as

$$\sigma = \sigma_0(1 - \theta) + \sigma' \theta \quad (4.1.6)$$

where σ_0 is the surface charge for the base electrolyte in the surface inactive solution (where $c_{org} = 0$), σ' is the surface charge density for the solution where the surface coverage $\theta = 1$. Using Eqs. (4.1.3) and (4.1.6) it is possible to obtain that

$$\sigma = C_0 E (1 - \theta) + C' (E_{\sigma=0} - E_N) \theta \quad (4.1.7)$$

where C_0 is the differential capacitance, when $\theta = 0$, C' is the differential capacitance, when $\theta = 1$, $E_{\sigma=0}$ is the zero charge potential and E_N is equal to the change in the zero charge potential value due to the displacement of a monolayer of water molecules by a monolayer of organic adsorbate. After differentiation of Eq. (4.1.7) with respect to E , we shall receive [1,7,8]

$$C = C_0(1 - \theta) + C' \theta + (\sigma' - \sigma_0) \frac{d\theta}{dE} \quad (4.1.8),$$

At the maximal adsorption potential (E_{max}) the derivative $d\theta/dE = 0$ and under these circumstances we can receive

$$C = C_0(1 - \theta) + C' \theta \quad (4.1.9).$$

The experimental surface coverage values at $E = E_{max}$ can be estimated using the Frumkin's model of the two parallel capacitors [1,7,8]

$$\theta = (C_0 - C) / (C_0 - C') \quad (4.1.10)$$

Thereafter, to a first approximation, usually the applicability of the Frumkin adsorption isotherm [8]

$$B_{\max} c_{\text{org}} = \frac{\theta}{1 - \theta} \exp(-2a\theta) \quad (4.1.11)$$

is assumed where B and a are the adsorption equilibrium constant and molecular interaction parameter at E_{\max} , respectively.

The surface pressure of the adsorbate film π , can be calculated by using the back-integration method based on Eq. (4.1.4) as follows

$$\pi(E) = \gamma'_{c=0} - \gamma'_c = \int_{E_0}^E \sigma_c dE - \int_{E_0}^E \sigma_{c=0} dE \quad (4.1.12)$$

where subscripts c and $c=0$ indicate the presence or absence of the adsorbate in the bulk of the base electrolyte, respectively [1–6,10–12].

The values of Γ and Γ_{\max} can be obtained according to the Eq. (4.1.13)

$$\Gamma = \frac{1}{RT} \left(\frac{\partial \pi}{\partial \ln c} \right)_{E, T, p} \quad (4.1.13)$$

Usually the values of Γ_{\max} are obtainable from the slope of the linear part of the π , $\log c_{\text{org}}$ dependences (constructed at $E = \text{const}$). Using the obtained Γ_{\max} and surface charge density values, we can calculate the Gibbs adsorption values according to the relation

$$\Gamma = \frac{\sigma_{\Gamma} - \sigma_{\Gamma=0}}{\sigma_{\Gamma_{\max}} - \sigma_{\Gamma=0}} \Gamma_{\max} \quad (4.1.14)$$

The values of $(\sigma_{\Gamma_{\max}} - \sigma_{\Gamma=0})$ can be obtained by the extrapolation of the linear section of the $\sigma(E)$ -curves.

The orientation of the adsorbate molecule, which is reflected in the molecular area S_A and can be correlated by Γ_{\max} (if Γ_{\max} corresponds to $\theta_{\max} = 1$) as

$$S_A = \theta_{\max}/\Gamma_{\max}N_A \approx 1/\Gamma_{\max}N_A \quad (4.1.15)$$

where Γ_{\max} is the maximum Gibbs excess for organic compound at the electrode surface; N_A is Avogadro's number. The experimental values of S_A can be compared with the projections of Courtauld models for vertical and flat orientations [25].

The standard Gibbs energy of adsorption ΔG_{ads}^0 at E_{\max} is obtained as [1–8]

$$\Delta G_{\text{ads}}^0 = -RT \ln (55.5 B_{\max}) \quad (4.1.16).$$

The Gibbs energy of total intermolecular interaction in the adsorption layer is obtained as [13,14,89,90]

$$-\Delta G_{\text{int}}^0 = 2aRT = 2Z_{W-A} - Z_{A-A} - Z_{W-W} \quad (4.1.17)$$

where Z is the particle-particle interaction energy, W stands for H_2O and A for adsorbate.

The experimental data to calculate the adsorption parameters of organic compounds adsorption at the metal electrodes have been obtained by the electrochemical impedance, cronocoulometric measurements method and STM study.

4.2. Adsorption kinetics of organic compounds

Frumkin and Melik-Gaikazyan first observed the frequency-dependence of the impedance of the Hg electrode adsorbing neutral organic molecules [3,9–18], this conception has been enlarged to other metal electrodes by various authors [1,2,19–22]. For the case of adsorption kinetics controlled entirely by the rate of diffusion, they deduced the following expressions for the frequency-related admittance of the electrode [3,9,–18]

$$C_p = C_{\text{true}} + \frac{C_{ad} \left[\left(\frac{\partial \Gamma}{\partial c} \right)_E \left(\frac{\omega}{2D} \right)^{1/2} + 1 \right]}{\left[\left(\frac{\partial \Gamma}{\partial c} \right)_E \left(\frac{\omega}{2D} \right)^{1/2} + 1 \right]^2 + 1} \quad (4.2.1)$$

$$\frac{1}{\omega R_p} = \frac{C_{ad} \left[\left(\frac{\partial \Gamma}{\partial c} \right)_E \left(\frac{\omega}{2D} \right)^{1/2} \right]}{\left[\left(\frac{\partial \Gamma}{\partial c} \right)_E \left(\frac{\omega}{2D} \right)^{1/2} + 1 \right]^2 + 1} \quad (4.2.2)$$

where Γ is surface concentration; μ is chemical potential; and ω is angular frequency equal to $2\pi f$; C_p is a parallel interfacial capacitance; $C_{true} = (\partial q / \partial E)_{\Gamma, \mu}$ is an interfacial capacitance as ac frequency $f \rightarrow \infty$, $C_0 = (\partial q / \partial E)_{\Gamma, \mu} + (\partial q / \partial \Gamma)_E (\partial \Gamma / \partial E)_\mu$ is a differential capacitance as $f \rightarrow 0$; and $C_{ad} = C_0 - C_{true} = (\partial q / \partial \Gamma)_E (\partial \Gamma / \partial E)_\mu$ is an adsorption capacitance, caused by the dependence of Γ (i.e. surface coverage θ) on E [9,10].

As shown by Armstrong et al. [11], if the diffusion controlled relaxation time ($\tau_D = 1/2\pi f_D$) is defined as

$$\tau_D = (\partial \Gamma / \partial c)_E^2 / D \quad (4.2.3)$$

and a Cole–Cole distribution [12] of relaxation times about τ_D is assumed (with the particular value $\alpha = 0.5$ in their Eq. (4.2.13) [12], which for the case of relaxation of dielectric polarization leads to the frequency dependence of the real ε' and imaginary ε'' parts of the complex dielectric constant ε^*) then Eqs. (4.2.1) and (4.2.2) can be rewritten as

$$C_p = C_{true} + \frac{C_{ad} \left[1 + (0.5\omega\tau_D)^{1/2} \right]}{1 + (2\omega\tau_D)^{1/2} + \omega\tau_D} \quad (4.2.4)$$

$$1/\omega R_p = \frac{C_{ad} (0.5\omega\tau_D)^{1/2}}{1 + (2\omega\tau_D)^{1/2} + \omega\tau_D} \quad (4.2.5)$$

Eqs. (4.2.4) and (4.2.5) require that $1/\omega R_p$ versus C_p (so called Cole-Cole plots) should take the form of a quarter-circle, intersecting the C_p -axis at the values C_{true} and $(C_{true} + C_{ad})$ [11–14].

For the case of adsorption kinetics controlled entirely by the rate of a heterogeneous charge transfer process, Frumkin and Melik-Gaikazyan [3, 9] deduced the following equations for the frequency-related admittance of the electrode:

$$C_p = C_{true} + \frac{C_{ad}(\partial\nu/\partial\Gamma)_{E,c}^2}{\omega^2 + (\partial\nu/\partial\Gamma)_{E,c}^2} \quad (4.2.6)$$

$$1/\omega R_p = \frac{C_{ad}(\partial\nu/\partial\Gamma)_{E,c}\omega}{\omega^2 + (\partial\nu/\partial\Gamma)_{E,c}^2} \quad (4.2.7)$$

where ν in $\text{mol cm}^{-2} \text{ s}^{-1}$ is the net rate of adsorption due to the departure from equilibrium conditions.

If

$$\tau_K = \left(\frac{\partial\Gamma}{\partial\nu} \right)_{E,c} \quad (4.2.8)$$

is defined as the relaxation time of the heterogeneous charge transfer (adsorption) process ($\tau_K=1/2\pi f_K$), then Eqs. (4.2.6) and (4.2.7) become

$$C_p = C_{true} + \frac{C_{ad}}{1 + \omega^2 \tau_K^2} \quad (4.2.9)$$

$$1/\omega R_p = \frac{C_{ad} \omega \tau_K}{1 + \omega^2 \tau_K^2} \quad (4.2.10)$$

Thus, according to [11, 14], the $1/\omega R_p$ versus C_p plot should take the form of a semi-circle with a centre $C_p=C_{ad}/2+C_{true}$; $1/\omega R_p=0$. Eqs. (4.2.9) and (4.2.10) have the same form as the Debye–Pellet equations for the relaxation in a dielectric with a single relaxation time [11, 12]. It should be noted that on the basis of the Frumkin adsorption isotherm, the following equations for the diffusion relaxation time

$$\tau_D = \frac{\Gamma_m^2 \theta^2 (1-\theta)^2}{c^2 D [1 - 2a\theta(1-\theta)]^2} \quad (4.2.11)$$

and for the adsorption relaxation time

$$\tau_K = \frac{\Gamma_m \theta (1-\theta)}{\nu_0 [1 - 2a\theta(1-\theta)]} \quad (4.2.12)$$

have been derived by Retter and Jehring [15] with the Frumkin interaction coefficient a , adsorption exchange rate ν_0 and Γ_{\max} , characterizing the influence of the maximal Gibbs adsorption and the surface coverage θ on the corresponding relaxation times. Therefore the intermolecular interaction energy plays a very big role in τ_D and τ_K values.

The situation of mixed diffusion and heterogeneous charge transfer control was studied in the most general case by Lorenz and Möckel [16–25]. The frequency-related admittance has been expressed by the relations

$$C_p = C_{true} + \frac{C_{ad} [1 + (0.5\omega\tau_D)^{1/2}]}{[(0.5\omega\tau_D)^{1/2} + \omega\tau_K]^2 + [(0.5\omega\tau_D)^{1/2} + 1]^2} \quad (4.2.13)$$

$$1/\omega R_p = \frac{C_{ad} [(0.5\omega\tau_D)^{1/2} + \omega\tau_K]}{[(0.5\omega\tau_D)^{1/2} + \omega\tau_K]^2 + [(0.5\omega\tau_D)^{1/2} + 1]^2} \quad (4.2.14)$$

If τ_K and τ_D are of the same order, the $1/\omega R_p$ versus C_p plot gives a gradual transition from a quarter-circle (at low ω when there is effectively complete diffusion control) to a semi-circle (at high frequencies when the control is effectively heterogeneous)[16,17].

According to the Lorenz model the impedance values for so-called adsorption branch in parallel to C_{true} can be calculated as [10,16,23]

$$Z_1' = (0.5\tau_D)^{1/2} \omega^{-1/2} C_{ad}^{-1} + \tau_K C_{ad}^{-1} \quad (4.2.15)$$

$$Z_1'' = (0.5\tau_D)^{1/2} \omega^{-1/2} C_{ad}^{-1} + (\omega C_{ad})^{-1} \quad (4.2.16)$$

If the diffusion is the limiting stage of an adsorption process, then the equilibrium values of differential capacitance at $\omega \rightarrow 0$ can be obtained by the linear extrapolation of the C_{ad} , $\omega^{1/2}$ -dependence to $\omega^{1/2}=0$, as well as being calculated by Eq. (4.2.17)

$$C_{ad}(\omega=0) = C_{ad}^2(\omega) R_p^2(\omega) \omega^2 + \{(C_{ad}(\omega) R_p(\omega) \omega - 1) R_p(\omega) \omega\}^{-1} \quad (4.2.17)$$

where $C_{ad}(\omega)$ and $R_p(\omega)$ are the values of the differential (additional) capacitance and parallel resistance at $\omega=\text{const}$ [18,19]. Thus, by linear extrapolation of the $R_S(\omega)$ -values to $\omega \rightarrow \infty$, the solution resistance $R_S(\omega)=R_{el}$ can be determined. Since the amount of organic compound added is small and does not affect the solution resistance, one can assume R_{el} to be equal to the ohmic component R_S of the impedance in the pure base electrolyte solution [3, 9].

If, at a given frequency, the adsorption process is characterized by the additional capacitance $C_{ad}(\omega)$ and by the parallel resistance $R_p(\omega)$, which are assumed to be parallel in the equivalent circuit, then for a slow diffusion step

$$\cot \delta = R_p(\omega)C_{ad}(\omega) = 1 + \sqrt{2D} / (\partial \Gamma / \partial c)_E / \sqrt{\omega} = 1 + M / \sqrt{\omega} \quad (4.2.18)$$

where M is the slope of the $\cot \delta$ vs $\omega^{-1/2}$ plots.

At very low frequencies noticeable deviations have been observed, explained according to Lorenz [16,23] and Damaskin et al. [1,13,14] by the two-dimensional association of the adsorbed molecules in the interfacial metal | solution region. In this case the value of $\cot \delta$ can be calculated as

$$\cot \delta = \frac{k_1 \left(k_2 + k_1 \frac{\sqrt{\omega}}{M} \right) + \left(\frac{\omega}{\omega_0} \right)^2 \left(k_3 + \frac{\sqrt{\omega}}{M} \right)}{\left[k_1^2 + \left(\frac{\omega}{\omega_0} \right)^2 \right] \left(\frac{\omega}{\omega_0} + \frac{\sqrt{\omega}}{M} \right) + \frac{\omega}{\omega_0} (k_1 k_3 - k_2)} \quad (4.2.19)$$

where ω_0 is the exchange rate of the two-dimensional association, and k_1 , k_2 and k_3 are certain constants characterizing the process of two-dimensional association [1,13,14,16,24].

Usually, the components of the adsorption impedance are calculated from the impedance data of the cell used for the measurements (series circuit), i.e. from $C_S(\omega)$ and $R_S(\omega)$ following the procedure described in Refs. [1,13,14, 18,19,23].

4.3. Phase transition in two-dimensional adlayers at electrode surface: thermodynamics, kinetics and structural aspects

Two-dimensional (2D) phase transitions on surfaces have received increased attention in recent years [24–27] as they are related in important aspects in surface, interfacial and materials science as well as nanotechnology, such as ordered adsorption, island nucleation and growth [25,28–30], surface reconstruction [31], and molecular electronics [32]. Also directly related to two-dimensional phase formation are some kinetic phenomena as catalytic activity, selective recognition of molecular functions [36], or chirality of surfaces [33–35].

Organic monolayer on well-defined metal substrates may be obtained by molecular beam epitaxy (MBE), so-called ‘self-assembled monolayers’ (SAM) or Langmuir-Blodgett (LB) films [36–55]. Alternatively, molecular and ionic

monolayer can also be obtained on conducting surfaces in an electrochemical environment. This approach offers the advantage that formation and properties of a wide variety of adlayer can be controlled as required by the applied electrode (substrate) potential and subsequently characterized by structure-sensitive in situ techniques in real space and real time. For these reasons potentiostatically or galvanostatically generated monolayers on well-defined metal electrodes have become attractive model systems and provide an important testing ground for fundamental issues in 2D physics and chemistry, such as phase transitions in adlayers and substrate surfaces [36–59].

Basic ordering principles of the above mentioned monolayers appear to be (1) the ability to create strong and intermolecular hydrogen bonds between adjacent molecules [49,50,54], (2) packing constrains, molecular geometry, and dipole forces [55], (3) ion pairing [56,57], (4) the formation of interfacial stacks due to π -electron attraction and London dispersion forces [48,50,51,52], (5) hydrophobic interaction [58], (6) substrate-adsorbate coordination chemistry [49,53].

The influence of the solvent on the formation and stability of 2D adlayers is unexplored and controversial [26,37]. Capacitance measurements of ordered 2-thiouracil film at mercury–acetonitrile interface shows that small amount of water shifts the stability range and saturation capacitance of the solidlike organic phase [59], while camphor measurement at Au(111) interface demonstrate that the organic adlayer is stabilized by hydrogen-bonded coadsorbed water species which represent the Helmholtz region by a network of two or three capacitors [1,60–63] and classical thermodynamics based on mean-field treatment [64–66].

Historically, Frumkin-type models were applied first to describe 2D phase transitions in organic adlayers at metal-electrolyte interface as function of concentration, potential and temperature. In the simplest case of one-step adsorption, the classical Frumkin isotherm (Eq. 4.1.11) degenerates into a vertical discontinuity if molecular interaction parameter $a \geq 2$ [60–62]. The latter is related to the average nearest-neighbor interaction energy as follows

$$\varepsilon_{AA} = -\frac{RTa}{2} \quad (4.3.1).$$

The derivation of a is based on the Bragg-Williams or Frumkin adsorption model (MFA) assuming (1) the homogeneous (statistical) distribution of molecules among energetically uniform sites, and (2) neglecting local fluctuation and correlation [40–42]. Retter pointed out that a more realistic isotherms treatment of 2D condensation in organic adlayer requires the consideration of localized adsorption and short-range (nearest-neighbor interaction) [67]. The so-called quasi-chemical approximation (QCA) considers nearest-neighbor site pairs, but treats them as independent of each other [38, 39]:

$$\ln(Bc) = \left[\left(\frac{(\beta - 1 + 2\theta)(1 - \theta)}{(\beta + 1 - 2\theta)\theta} \right)^2 \frac{\theta}{1 - \theta} \right] \quad (4.3.2)$$

$$\beta = \left[1 - 4\theta(1 - \theta) \times \left(1 - \exp\left(\frac{a_{Oc}}{2} \right) \right) \right]^{1/2} \quad (4.3.3).$$

The LTSE (low-temperature series expansion model) [68] considers equilibrium adsorbate clusters (up to 15 monomers) as well as various configurations of clusters with constant size indication that the lattice geometry is taken into account. The corresponding isotherm of the condensed phase for the square lattice is given by

$$\theta = 1 - x^8 z^{-1} - 2 \left(2x^{14} - \frac{5}{2x^{16}} \right) z^{-2} - 3 \left(6x^{20} - 16x^{22} + \frac{31}{3x^{24}} \right) z^{-3} \dots \quad (4.3.4)$$

with $z=Bc$ and $x=\exp(-a_{LTE}/4)$. Equation (4.3.4) represents truncated series expansion, which is obtained by the assumption that contributions of clusters larger than trimers can be neglected.

The degree of surface coverage of the condense phase can be determined experimentally at constant potential from the saturation capacitance C_{sat} , the capacitance of the noncondensed phase C_0 , and the capacitance of the film C_{film} according to [68, 69]

$$\theta = \frac{C_0 - C_{film}}{C_0 - C_{sat}} \quad (4.3.5)$$

The potential dependences of θ at constant concentration results from combining the respective isotherms (4.1.11), (4.3.2) or (4.3.4) with the potential dependence of adsorption equilibrium constant B of neutral organic molecules on metal-solvent electrolyte interface, which is defined as [1, 68]

$$B = B_{max} \exp(-\alpha(E - E_{max})^2) \quad (4.3.6)$$

$$B_{max} = \left(\frac{1}{55.5} \right) \exp\left(\frac{\Delta G_A^0}{RT} \right) \quad (4.3.7)$$

$$a = \frac{C_0 - C_{sat}}{2RT\Gamma_{max}} \quad (4.3.8)$$

with E_{\max} , B_{\max} , ΔG_A^0 represented the electrode potential at maximum adsorption, the adsorption coefficient at $E=E_{\max}$, and the Gibbs energy of adsorption. These equations (Eqs. 4.3.5–4.3.8) and isotherms permit to model capacity versus potential dependences in the region of 2D condensation.

The kinetics of 2D phase formation in the simplest case involves the mass transport of the molecules/ions from the bulk electrolyte toward the surface, adsorption and/or charge transfer and adsorption at the electrode surface. Mass transport controlled by diffusion in the case of semi-infinite linear diffusion, is obtained from Fick's first law according to

$$\Gamma(t) = \int_0^t D \left(\frac{\partial c}{\partial x} \right)_{x=0} dt \quad (4.3.9)$$

with x as the distance from the plane of adsorption at the electrode. If the rate of diffusion is sufficiently high, so that the surface concentration is zero $c_x=0$ during the phase formation

$$\theta = \frac{\Gamma}{\Gamma_{\max}} = \frac{2c}{\Gamma_{\max}} \sqrt{\frac{Dt}{\pi}} \quad (4.3.10)$$

Γ_{\max} is the maximum surface excess on the condensed phase [43, 44]. Diffusion-controlled adsorption in the frequency domain was treated theoretically and experimentally by Melik-Gaikazyan [3, 9], Lorenz [16,23], and Armstrong [11].

The kinetics of the adsorption step in the absence of mass transport control was treated by Lorenz [16] and Delahay [45]. The former yields, in the limit of a negligible rate of desorption,

$$\theta = 1 - \exp(-k_{ad} c_{x=0} t) \quad (4.4.11)$$

where k_{ad} is the adsorption rate. The same treatment is also valid for interfacial faradaic reaction.

Lorenz [23] combined diffusion, intrinsic adsorption, and surface association as separate contributions and developed the first model attributes a slow (dynamic) adsorption step to the 2D association of adsorbed species at an electrode interface.

The kinetics of 2D phase formation and dissolution of organic adlayer are analyzed on the basic macroscopic models. Recently modern in situ techniques such as STM and time-resolved infrared spectroscopy (SEIRAS) were applied to study structural aspects of these phase transitions at a molecular or atomic level [26,27,50].

4.4. Fitting of impedance data of two-dimensional adlayers

Experimental impedance data were mainly analyzed using the equivalent circuits illustrated in Fig. 1, where R_{el} is the electrolyte resistance, C_{true} and C_{ad} are the double layer and adsorption capacitances, respectively; CPE is the constant phase element; Z_W is Warburg-like diffusion impedance, R_{ad} is the adsorption or partial charge transfer resistance and R_{ct} is charge transfer resistance [1, 9–11, 19, 20, 70–83]. C_n and R_n are the capacitance and resistance of the “needle” adsorption-desorption peak formation discussed later in more detail. The value of C_{true} characterizes the capacitance of the metal | electrolyte interface at $\omega \rightarrow \infty$ and C_{ad} is caused by the dependence of the electrode surface coverage θ on the electrode potential E . There are two accurate ways to obtain an indication of how well the modelling function reproduces the experimental data set: (1) observing the parameter values and their relative error estimates (in %); (2) the chi-square function (χ^2) and the weighted sum of the squares (Δ^2) also give a good indication about the quality of the fit [1, 5, 19, 20, 70, 72–75].

For adsorption of neutral organic molecules at electrode surface in aqueous system to the first approximation the classical Frumkin-Melik-Gaikazyan (FMG) equivalent circuit (presented in Fig. 1 (circuit b)) is valid. In this case, the specific impedance and capacitance functions have the following forms

$$Z(\omega) = R_{el} + \frac{1}{j\omega C_{dl} + \frac{1}{\frac{\sigma_{ad}}{\sqrt{j\omega}} + \frac{1}{j\omega C_{ad}}}} \quad (4.4.1)$$

and

$$C(\omega) = \frac{1}{j\omega[Z(\omega) - R_{el}]} = C_{dl} + \frac{C_{ad}}{1 + \sigma_{ad} C_{ad} \sqrt{j\omega}} \quad (4.4.2)$$

where $\sigma_{ad}(j\omega)^{-1/2}$ represents the diffusion (Warburg-like) impedance Z_W with its coefficient σ_{ad} .

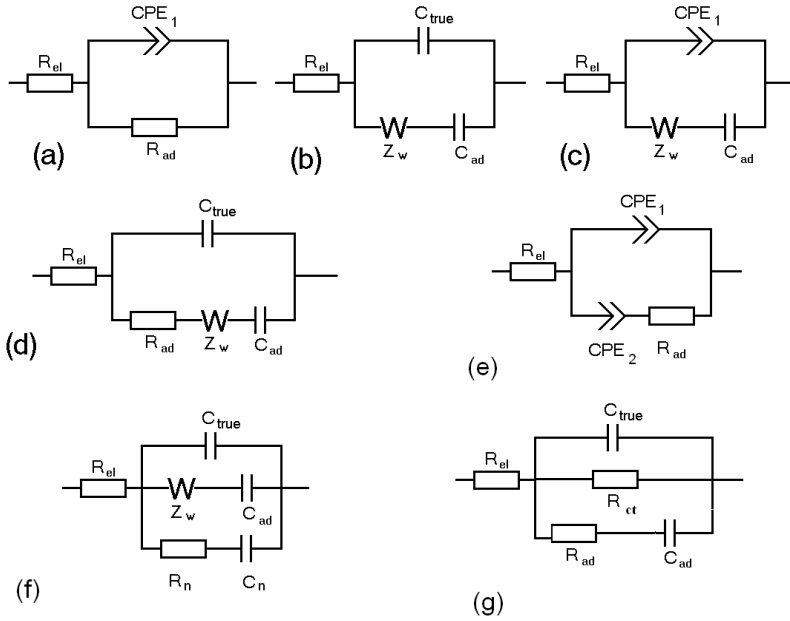


Fig. 1. Equivalent circuits of an electrode in 0.05M Na₂SO₄ aqueous solution (a) and with addition of organic compounds: (b) Frumkin-Melik-Gaikazyan (FMG); (c) modified Frumkin-Melik-Gaikazyan circuit, where the “true” capacitance ($C_{\text{true}} \equiv C$ at $\omega \rightarrow \infty$) has been replaced by the CPE₁ (FMGC₁); (d) Frumkin-Melik-Gaikazyan and Randles circuit; (e) modified Randles circuit where CPE₁ and CPE₂ are taking into account the nonhomogeneous adsorption layer; (f) Wandlowski de Levie; (g) modified Dolin-Ershler circuit where R_{ct} is additional parallel charge transfer resistant, caused by the irreversible faradaic reaction.

According to the model developed by Wandlowski and de Levie [57, 78–80], the isotropic two-dimensional cluster will mostly grow at its periphery where the rate of growth is proportional to the interfacial adsorbate concentration Γ on that part of the interface which is not yet covered by clusters, and on the periphery length $2\pi r$ with a proportionality constant k_g (i.e. k_g is the rate constant of the cluster growth). The rate constant of the reverse process (i.e. edge dissolution) is defined as k_d . However, the growth and dissolution of cluster will be assumed to have another pathway available as well, i.e. for the cluster | electrolyte interface the rate constants k_g' and k_d' are assumed. Under these conditions the following expression for the cluster formation rate is valid [79]

$$\frac{dS}{dt} = 2\pi r(k_g \Gamma - k_d) + \pi r^2(k_g' c_{\text{cat}} - k_d') \quad (4.4.3)$$

where S is the area of the cluster, t is time, Γ is the (absolute) interfacial excess, and c_{cat} is the adsorbate concentration, here assumed to be uniform up to the interface. Thus, according to this model, the interface is composed of areas covered by clusters, and other areas not so covered, with the charge densities σ_1 and σ_0 , respectively [79]. The charge density of the electrode, σ , is given by

$$\sigma = \sigma_0(1 - \theta) + \sigma_1\theta \quad (4.4.4)$$

and current density j is given by

$$j = d\sigma/dt = (\sigma_1 - \sigma_0)d\theta/dt + (1 - \theta)d\sigma_0/dt + \theta d\sigma_1/dt \quad (4.4.5)$$

As shown in [79], the first term of Eq. 4.4.5 describes the dominant features of the needle peak at low frequencies. The sinusoidal perturbation of the potential can be expressed as $E = E' + E''e^{j\omega t}$, (where j is imaginary unit ($\sqrt{-1}$), ω angular frequency and t time) the cluster radius as $r = r' + r''e^{j\omega t}$, the cluster area as $S = S' + S''e^{j\omega t}$, the interfacial adsorbate concentration as $\Gamma = \Gamma' + \Gamma''e^{j\omega t}$, the extended area fraction as $\theta_x = \theta_x' + \theta_x''e^{j\omega t}$, the area fraction as $\theta = \theta' + \theta''e^{j\omega t}$, and the current density as $j = j' + j''e^{j\omega t}$. Thus, according to [79] the current density of the needle adsorption-desorption peak is given as

$$j_n = j_n' + j_n''e^{j\omega t} \quad (4.4.6)$$

and

$$\begin{aligned} j_n'' &= j\omega(\sigma_1 - \sigma_0)\theta'' = j\omega(\sigma_1 - \sigma_0)e^{-\theta_x'}\theta_x'' \\ &= j\omega(\sigma_1 - \sigma_0)e^{-\theta_x'}4\pi k_g(\partial\Gamma/\partial E)E''\sum r'/(2j\omega - k_g'c + k_d') \end{aligned} \quad (4.4.7)$$

from which the impedance of the needle adsorption-desorption peak can be calculated as [79]

$$Z_n = E/j_n'' = (2j\omega - k_g'c + k_d')/\{j\omega(\sigma_1 - \sigma_0)e^{-\theta_x'}4\pi k_g(\partial\Gamma/\partial E)\sum r'\} \quad (4.4.8)$$

Thus, impedance of the needle peak can be expressed by a series combination of formation resistance (R_n) and capacitance (C_n), of the needle peak (Fig. 1, circuit f)

$$R_n = 1/\{(\sigma_1 - \sigma_0)e^{-\theta_x'}4\pi k_g(\partial\Gamma/\partial E)\sum r'\} \quad (4.4.9)$$

$$C_n = \{(\sigma_1 - \sigma_0)e^{-\theta_x'}4\pi k_g(\partial\Gamma/\partial E)\sum r'\}/(k_d' - k_g'c) \quad (4.4.10)$$

For dilute solutions of organic compound demonstrating ability to form the 2D condensation layer, the diffusion effects are not yet completely negligible and therefore it must be introduced the time-dependent interfacial concentration (i.e. surface concentration depends on ac frequency) in the form $c = c' + c''e^{j\omega t}$ and

$$\Gamma'' = (\partial\Gamma/\partial E)E'' + (\partial\Gamma/\partial c)c'' \quad (4.4.11)$$

Thus, there is a difficulty in that the boundary condition defining the interfacial flux will now be heterogeneous, and there is no exact solution for this non-trivial problem yet [79]. It is reasonable that the effect of diffusion is likely to be stronger for the non-covered interface than the covered part, because slow dissolution and growth are reducing its effects at the patches [79] (Fig. 1, circuit f). The interfacial admittance can then be represented approximately by the equivalent circuit, where the Frumkin-Melik-Gaikazyan model for the interface non-covered by the two-dimensional compact cluster is valid. As shown in paper [II] for less concentrated solutions the role of two-dimensional compact clusters is small and the circuit simplifies to the classical Frumkin-Melik-Gaikazyan model discussed in Refs. [I, 5, 9–11, 13, 19, 20,71].

5. EXPERIMENTAL

The adsorption of uracil, tetrabutylammonium cations, camphor, sodium dodecyl sulfate and 2, 2'-bipyridin on the single Bi(111), Bi(001) and Bi(01 $\bar{1}$) planes has been studied by the ac impedance, chronocoulometry and cyclic voltammetry method. The final surface preparation of Bi electrodes was obtained by electrochemical polishing in an aqueous KI+HCl solution. Thereafter, the electrodes were very well rinsed with ultra purified water and polarized at -1.0 V (vs. Ag/AgCl/KCl saturated solution in H₂O) in the surface-inactive solution for 2 h. The impedance was measured using an Autolab PGSTAT 30 with a FRA 2 ($0.1 < f < 10\ 000$ Hz, 5 mV modulation), and the system was calibrated using various standard equivalent circuits. The quality of the electrodes was tested by X-ray diffraction as well as AFM and STM methods [I-VI].

The water for preparing the solutions was treated with the Milli Q+ purification system (resistance > 18.2 M Ω cm). Solutions were prepared volumetrically using Na₂SO₄ purified by triple recrystallization from water, and treated in vacuum to dryness. Na₂SO₄ was calcined at 700°C immediately prior to preparing the solutions. Electrolytic hydrogen was bubbled for 1–2 h through the electrolyte before the submersion of the electrode into the solution and the temperature was kept at 298 ± 0.1 K. Compounds studied were obtained from the company Aldrich.

6. RESULTS AND DISCUSSION

6.1. Adsorption of uracil on bismuth single crystal planes [I, III]

The electrochemical impedance spectroscopy method has been used for the quantitative study of uracil adsorption kinetics at the bismuth single crystal plane | aqueous Na_2SO_4 solution interface. The shape of the Z'' , Z' -plots (Fig. 2) depends noticeably on the electrode potential as well as somewhat on the plane structure [I] and on the concentration of organic compound in the solution. At fixed c_{org} and Z' , the value of $|Z''|$ is maximal in the region of electrode potentials $-1.1 < E < -0.6$ V (Ag|AgCl), i.e. in the region of maximal adsorption. In this region of potentials the impedance spectra have complicated shape and can be fitted by tilted non-linear lines rather than by the depressed semicircles. At small ac frequency, the so-called capacitive behaviour prevails in the region of maximal adsorption $-1.0 < E < -0.5$ V (Ag|AgCl). At E_{max} , differently from Bi(*hkl*) | tert-PenOH, n-HepOH, cyclohexanol (CH) and D-ribose interfaces [2,19,20,70,81], the shape of the Z'' , Z' -plots depends noticeably on concentration of the organic compound in solution, and the values of R_0 (R_0 is the real impedance component Z' at $\omega \rightarrow 0$) are somewhat higher for the more concentrated uracil solutions [I]. At the electrode potentials $E < -1.1$ V (Ag|AgCl), the Z'' , Z' -plots can be simulated to a very rough approximation by the depressed semicircles with the centre displaced below the real axis, indicating that the relaxation time τ is not a simple-valued quantity but is distributed continuously or discretely around a mean $\tau_m = \omega_m^{-1}$ value [3,13,14, 72–77]. Thus, according to experimental data, two limiting stages (diffusion and adsorption or the partial charge transfer process [2,19,20,70,81]) seem to be valid at the Bi | 0.05 M Na_2SO_4 + uracil solution interface at $E < -1.1$ V (Ag|AgCl).

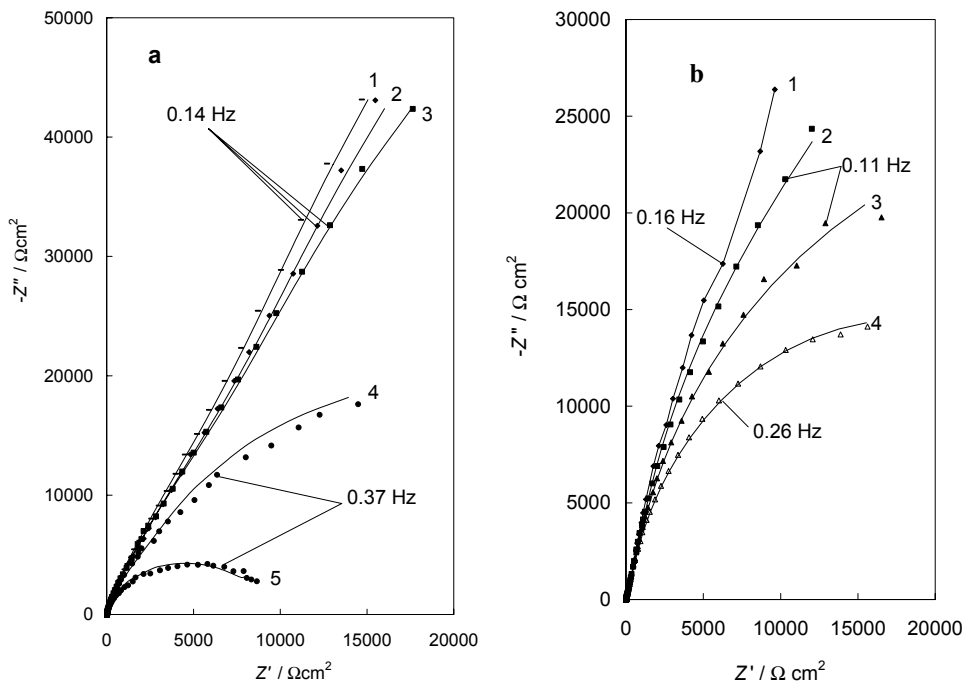


Fig. 2. Complex plane plots for Bi(111)|0.05M Na₂SO₄ + 30mM uracil (a) system at different electrode potentials, E/V vs Ag|AgCl: -0.9 (1); -0.7 (2); -1.0 (3); -1.1 (4) and -1.2 (5) and (b) at different uracil concentrations c : 30mM (1); 20mM (2); 8mM (3) and 0mM (4) at electrode potential $E=-1.1$ V vs Ag|AgCl (marks – experimental data; solid line – calculated according to FMG)

The shape of δ , $\log f$ -curves is practically independent of electrode potential if $E > -1.1$ V (Ag|AgCl). According to the experimental data (Fig. 3), the $|\delta|$ values for Bi(111)|uracil interface have a first maximum (so-called higher frequency maximum (HF)) at $f \approx 1 \times 10^2$ Hz and a second maximum at $f < 0.8$ Hz [I]. The maximal values of $|\delta|$ are practically independent of c_{org} at maximal adsorption potential if $f \geq 1.0$ Hz. The values of $|\delta|$ higher than 70° at $E > -1.3$ V (Ag|AgCl) indicate that, in this region of potentials, the Bi(hkl) | 0.05 M Na₂SO₄ + c M uracil interface can be simulated as a nearly ideally polarizable interface, where the deviations toward mixed kinetics (slow adsorption and diffusion steps) are possible [1,2,19,20,70,81]. The existence of two maxima in the δ , $\log f$ dependences indicates that two experimental relaxation times can be obtained, however this effect (i.e. two maxima in the δ , $\log f$ -plot) is not so well expressed for the Bi(01 $\bar{1}$)|uracil + 0.05 M Na₂SO₄ interface as for Bi(111) plane [III]. At very low frequencies $|\delta|$ decreases somewhat, which may be connected with the two-dimensional association [23] or with the partial charge

transfer between uracil and the Bi surface (or by a very slow faradaic process). At $E < -1.3$ V, the region of intensive decrease of $|\delta|$ with f is shifted toward higher values of f with the increase of negative polarization (Fig. 3). These results are in a reasonable agreement with the data for the Bi(hkl)|organic compound + Na₂SO₄ [2,19,20,70,81] and Hg|aliphatic alcohol interfaces [3,11,13,14].

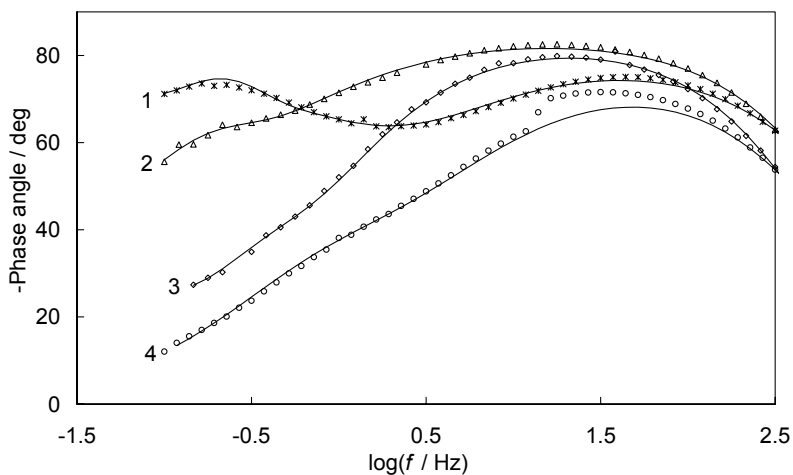


Fig. 3. Dependence of phase angle (δ) on ac frequency (f) for Bi(111) (1, 4) and Bi(011̄) (2, 3) in the aqueous 0.05M Na₂SO₄ solution with the addition of 30mM uracil at the electrode potentials -0.7 V(1, 2) and -1.2 V (3, 4) (marks-experimental data; solid lines-results calculated according to FMGC₁).

6.1.1. Simulation of impedance data

Experimental impedance data [I] were mainly fitted using the equivalent circuits illustrated in Fig. 1, and described in chapter 4.4. Non-linear regression analysis of Z'' , Z' -curves shows that, for less concentrated uracil solutions ($c_{\text{uracil}} < 2 \times 10^{-3}$ M) within the frequency range from 10 to 6000 Hz and in the region of uracil adsorption, these data can be simulated with the reasonable accuracy by classical Frumkin-Melik-Gaikazyan (FMG) equivalent circuit (circuit b in Fig. 1) [I,3]. However the modified Frumkin-Melik-Gaikazyan equivalent circuit [I] (Fig. 1 circuit c) (taking into account the inhomogeneous semi-infinite diffusion) can be used for fitting other experimental Z'' , Z' -plots at $c_{\text{uracil}} \geq 2 \times 10^{-3}$ M. Thus, to a first approximation, it can be concluded that the deviation of studied system from the classical Frumkin-Melik-Gaikazyan model arises because of the increase of surface coverage and compactness of the adsorption layer on the Bi surface. This effect has been observed for more complicated systems and can probably be explained using the theory of the electrochemical impedance of

anomalous diffusion [82–85] (i.e. using the anomalous diffusion model with a reflecting bounding interface in our case; $\alpha_{\text{org}} > 0.5$).

The values of the diffusion resistance R_D (at $\alpha_{\text{org}} = 0.5$ (FMG) as well as $\alpha_{\text{org}} \neq 0.5$) obtained according to Eqs. (4.4.1) and (4.4.2) are maximal in the region of maximal adsorption. Thus, R_D increases with the increase of surface coverage on Bi(*hkl*) electrodes at $c_{\text{org}} = \text{const}$. R_D depends somewhat on the plane studied, and increases from Bi(111) to Bi(01 $\bar{1}$). R_D has minimal values at the potentials $E \ll E_{\sigma=0}$, practically independently of the plane studied [I].

C_{ad} values calculated according to Eqs. (4.4.1) and (4.4.2) have minima at the potentials of maximal adsorption in a good agreement with the Frumkin-Damaskin adsorption theory of neutral organic compounds at ideally polarizable electrodes [1,3,9–14]. The C_{ad} values increase very quickly with the decrease of E in the region $E < -1.3$ V (Ag|AgCl), where the value of $(\partial\theta/\partial E)_{\mu}$ is high. At very high ω values as well as in the region of maximal adsorption, C_{ad} has a tendency to approach zero [I].

The dependence of C_{true} on the electrode potential is in a good agreement with the Frumkin-Damaskin adsorption theory of neutral organic compounds at the ideally polarizable electrodes [1–3,13,14]. C_{true} has minimal values in the region of zero charge potential (in the region of maximal adsorption) and increases quickly with desorption of the organic compound from the electrode surface with the increasingly negative polarization of the electrode [I].

6.1.2. Estimation of limiting stages [I]

The so-called Cole-Cole plots (frequency-related admittance) plots have been calculated (Fig. 4) according to Eqs. (4.2.5), (4.2.10) and (4.2.14). There is considerable deviation of the $1/\omega R_p$, C_p -plots from the quarter-circle (the purely diffusion-limited stage) as well as from the semi-circle (i.e. from the purely adsorption-limited process). The values of $\tau_{\text{exp}} = (2\pi f_{\text{max}})^{-1}$ obtained from Cole-Cole plots characterize the kinetically mixed-controlled adsorption process of uracil at the Bi(01 $\bar{1}$) | 0.05 M Na₂SO₄ interface [I]. Thus, in the region of higher frequencies ($1000 < f < 7000$ Hz), the values of depression angle β are noticeably lower than 45° indicate mixed kinetics of the uracil adsorption at the Bi planes [I,9–21]. For Bi(01 $\bar{1}$) at moderate frequencies ($10 < f < 100$ Hz) and at $E \geq -1.1$ V (Ag|AgCl), the values of the depression angle between the radius of the arc and the C_p -axis β' are noticeably higher than those at $f > 1000$ Hz and indicate that, in the region of lower ac frequencies, the deviation from the diffusion limitation is small as for this region of f the $1/\omega R_p, C_p$ -dependence can be simulated by a quarter-circle with a centre lying noticeably lower than the C_p -axis [I]. In the region of maximal adsorption in the case of very low

frequencies, an additional semicircle has been established for the Bi(111)|uracil interface, which is caused by the restructuring effects (probably two-dimensional association) prevailing in the adsorption layer at $f \leq 35$ Hz. For Bi(01 $\bar{1}$) plane, the linear dependence of $(\omega R_p)^{-1}$ on C_p with the angle $\beta'' \approx 45^\circ$ has been established (nearly the diffusion-like limited process). The slope of $1/\omega R_p$, C_p -dependences is noticeably lower ($\beta'' \approx 40^\circ$) in the low frequency region ($f < 44$ Hz) than at $f > 1000$ Hz and, thus, the deviation of the Bi(hkl)|uracil + Na₂SO₄ interface from the purely diffusion-limited mechanism is noticeably lower than at higher frequencies. According to the data in Fig. 4, the shape of the $1/\omega R_p$, C_p -curve depends very slightly on the concentration of uracil (if $-1.3 < E < -0.5$ V), and the values of $C_{\text{true}} \equiv C_p(\omega \rightarrow \infty)$ are practically independent of c_{uracil} [3].

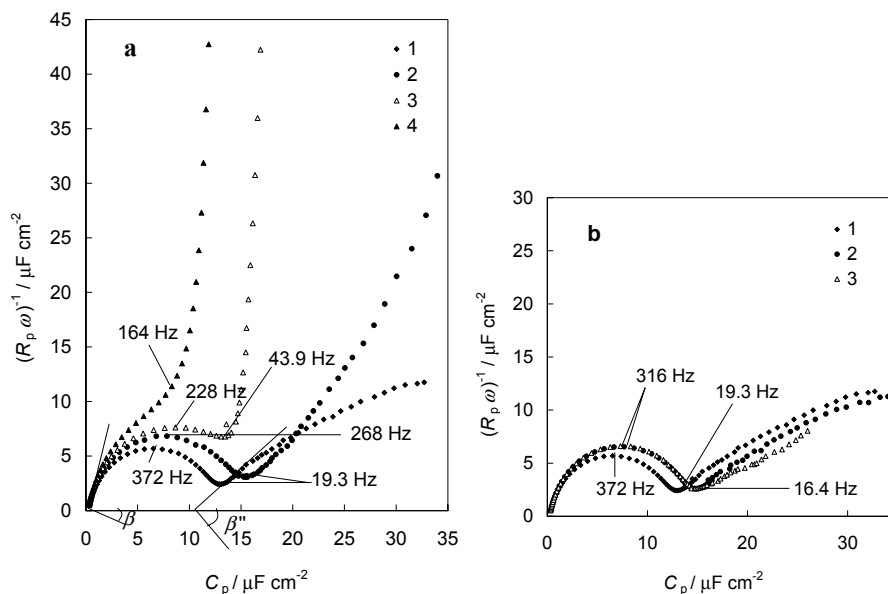


Fig. 4. Cole-Cole plots for Bi(111) in the 0.05M Na₂SO₄+ 30mM uracil solution at electrode potentials E/V (a) vs Ag|AgCl: -0.7V (1); -1.1 V(2); -1.4V (3); and -1.6V (4) and for (b) at $E=-0.7V$ with addition of uracil: 30mM (1); 20mM (2) and 8mM (3)

The values of relaxation frequency at $c_{\text{uracil}} > 1.0 \times 10^{-2}$ M depend noticeably on the electrode potential, and the values of τ_{exp} decrease with the decrease of the negative electrode potential, i.e. with the compactness of the uracil adsorption

layer [I]. The deviation of the system from diffusion limitation in the region of moderate frequencies is noticeable, and the values of the experimental relaxation time do not correspond to the diffusion relaxation times [I]. The values of τ_{exp} depend somewhat on the crystallographic structure studied. In the region of maximal adsorption noticeable increase in the $(\omega R_p)^{-1}$ values has been observed at very low frequencies ($f < 10$ Hz), which is caused by the slow reorganisation of the adsorption layer (two-dimensional association according to Lorenz and Möckel [1,13,14,16,23]).

As shown by Armstrong *et al.* [11], if the function

$$\log \left(\frac{(C_0 - C_p)^2 + (\omega R_p)^{-2}}{(C_p^*)^2 + (\omega R_p)^{-2}} \right) \equiv y^* \quad (6.1.2.1)$$

is plotted against $\log f$, a straight line with a slope value equal to $2(1-\alpha^*)$ should be observed. A linear dependence with the slope equal to unity (corresponding to $\alpha^* = 0.5$) for completely diffusion control process, and a straight line with a slope equal to 2 ($\alpha^* = 0$) for a completely heterogeneous charge transfer controlled process would be expected [11]. For mixed control, y^* vs. $\log f$ -dependence with unit slope at low frequencies would deviate to slope 2 at higher frequencies. The experimental data, indicate that the deviation of the Bi(*hkl*) | uracil system from diffusion control is smallest for the chemically most active Bi(01 $\bar{1}$) plane, for which the Gibbs adsorption values are lower than for Bi(111) plane [III]. The values of τ_{exp}^* (obtained from y^* , $\log f$ dependence [11]) are practically independent of c_{org} if $E < -1.1$ V (Ag|AgCl), but in the region of maximal adsorption τ_{exp}^* increases with the decrease of c_{org} in solution, being somewhat lower than the values of τ_{exp} , obtained from the Cole-Cole plots [I].

The experimental $(\omega R_p)^{-1}$, $\log f$ -dependences have been simulated using Eqs. (4.2.5), (4.2.10) and (4.2.14). According to the results of calculations, a better fit of the experimental and calculated data was established when Eq. (4.2.14) (mixed kinetics) was used [1,13,14,16,23]. The values of $\tau_{\text{D}}^{\text{theor}}$ and $\tau_{\text{K}}^{\text{theor}}$, indicate that the adsorption process is limited mainly by the heterogeneous adsorption step as the smaller values of $\tau_{\text{D}}^{\text{theor}}$ than $\tau_{\text{K}}^{\text{theor}}$ were established.

6.1.3. Adsorption isotherms and thermodynamic adsorption parameters [III]

The thermodynamics of uracil adsorption at Bi(*hkl*) has been studied using impedance spectroscopy method. The limiting adsorption potential shift E_{N} , Gibbs energy of adsorption $-\Delta G_{\text{ads}}^0$ and interaction constant values a in the

Frumkin isotherm have been calculated (Table 1) and compared with the corresponding data for other organic compounds studied by us [II, V, VI].

Table 1. Adsorption parameters for different systems [II, V, VI].

Compound	Plane	a	ΔG_{ads}^0 (kJmol ⁻¹)	C' (μFcm ⁻²)	$\Gamma_{\text{max}} \times 10^{10}$ (mol cm ⁻²)	S_{A_2} (nm ²)	E_N (V)	ΔG_{int}^0 (kJmol ⁻¹)
uracil	Bi(111)	1.5	-16.4	15.2	2.2	0.075	-0.05	-7.4
	Bi (01 $\bar{1}$)	1.1	-17.1	15.1	2.3	0.072	-0.07	-5.4
Dodecyl sulfate anion	Bi(111)	0.63	-27.5	5.53	1.11	0.15	0.053	-3.1
	Bi (01 $\bar{1}$)	0.81	-26.5	4.36	1.78	0.093	0.043	-3.9
	Bi(001)	0.75	-25.3	5.48	1.79	0.092	0.108	-3.7
camphor	Bi(111)	1.89	-21.1	3.2	3.4*	0.048	-	-9.5
2,2'- bipyridine	Bi(111)	1.45	-29.8	2.7	8.3*	0.020	-	-6.9

*calculated from *in situ* STM data.

The equilibrium capacitance C vs. E -curves have been obtained by the linear extrapolation of the $C_s, \omega^{1/2}$ -curves to the condition $\omega^{1/2}=0$. At constant ac frequency and in the region of maximal adsorption, C decreases with increasing c_{org} in solution. Differently from Bi(hkl)/ n -heptanol (n -HepOH), *tert*-pentanol (*tert*-PenOH) and cyclohexanol (CH) interfaces [2,19,20,89,90], there is no very well developed adsorption-desorption peaks in C, E -curves at the surface charge density $\sigma \ll 0$ and C starts to increase with increasing the negative polarization of the electrode at only $E < -1.5$ V (Ag|AgCl). Going further in the positive direction, the differential capacitance decreases to a value much smaller than that observed for the base electrolyte C_0 . The limiting capacitance C' (Table 1), obtained by the linear extrapolation of the $C^{-1}, c_{\text{org}}^{-1}$ - dependence to the

condition $c_{\text{org}}^{-1}=0$ [1–3,13,14,III–VI], increases from Bi(01 $\bar{1}$) to Bi(111) at the potential of maximal adsorption E_{max} .

The σ, E -curves for the Bi(hkl) | solution interface were obtained by integration of the C, E -curves, starting from the potential of zero charge $E_{\sigma=0}$ [III]. The values of $E_{\sigma=0}$ for different Bi single crystal planes were obtained from the position of the diffusion layer minimum in the C, E -curves for independently measured differential capacitance curves for dilute base electrolyte solutions (0.002M Na₂SO₄) and for 0.002M Na₂SO₄ M+ x M uracil solutions [III]. The negative surface charge density increases with the negative polarisation of the Bi(hkl) electrode surface but the experimental σ, E -curves for Bi(01 $\bar{1}$) in the more concentrated uracil solutions do not coincide with the σ, E -curve for the base electrolyte solution at $\sigma \ll 0$ as it was found for Bi(111) and for the other neutral organic compounds on Bi(hkl) in the previous works [2,19–22,70,89,90,86,87]. Therefore the σ, E -dependences for more concentrated uracil solutions were extrapolated to more negative potentials to coincide those with the σ, E -curve for the base electrolyte. It should be noted that the σ values in the case of c_{org} higher than 1×10^{-3} M at $E < -1.1$ V are not very exact, taking into account the mixed kinetic mechanism of adsorption. For that reason, it is impossible to obtain the exact Gibbs adsorption values and only the approximate values of $\Gamma_{\text{max}} \approx 2.2$ mol cm⁻² for Bi(111) and $\Gamma_{\text{max}} \approx 2.3$ mol cm⁻² for Bi(01 $\bar{1}$) have been obtained from the surface pressure π vs $\log c_{\text{org}}$ dependences according to the method discussed in [1–3, 13, 14, 30, 89, 90].

The limiting adsorption potential values E_N were obtained, presented in Table 1. The E_N negative values indicating that, differently from the simple aliphatic organic compounds [2,70,86,87,89,90], the uracil adsorption is characterized by the very small change in the dipole potential drop in the adsorbed layer at the Bi(hkl) surface.

The applicability of Frumkin adsorption isotherm was tested using the $\log[\theta/(1-\theta)c]$, θ -plots method. These plots have a good linearity within the region $0.1 \leq \theta \leq 0.8$ for Bi(111) and Bi(01 $\bar{1}$) planes and the Frumkin model is valid [III,2,19,20,86,87,89,90].

It was found that $-\Delta G_{\text{ads}}^0$ increase in the order Hg < Bi(111) < Bi(01 $\bar{1}$). The values of a are higher for Bi(hkl) compared with Hg [4, 91] indicating the noticeably higher surface activity of uracil and van der Waals intermolecular interaction energy on Bi(hkl) in comparison with the Hg electrode. The limiting adsorption potential shift are comparable for the Hg and Bi(hkl) electrodes, indicating the similar orientation of uracil molecules at Bi(hkl) planes and Hg electrode [4, 91].

6.2. Adsorption of sodium dodecyl sulfate on bismuth single crystal planes [VI]

Electrochemical impedance spectroscopy has been employed for the study of sodium dodecyl sulfate (SDS) and adsorption kinetics at the Bi(111), Bi(001) and Bi(01 $\bar{1}$) | 0.05 M Na₂SO₄ aqueous solution interface. The shape of Nyquist plots (Fig. 5) depends noticeably on the SDS concentration (c_{SDS}) as well as on the electrode potential, and somewhat on the plane studied. At potentials more negative than the adsorption–desorption peak potential ($E^{\text{peak}} \leq -1.4$ V vs. Ag/AgCl), the Z'' , Z' plots for all c_{SDS} studied can be represented by very well depressed semi-circles with experimental relaxation frequency $\tau_m = (\omega_m)^{-1} = (2\pi f)^{-1}$, which corresponds to mixed kinetics (i.e. the SDS adsorption process is limited by the slow adsorption (τ_K^{theor}) and diffusion (τ_D^{theor}) steps) [I,VI,2,11,13,14,16,23]. At potentials less negative than the potential of maximal adsorption E_{max} , the Z'' , Z' plots can be represented by the slightly depressed semi-circles again in all the regions of adsorbate concentration in 0.05 M Na₂SO₄ solution. The complicated shape of the Z'' , Z' plots at $c_{\text{SDS}} \geq 8 \times 10^{-4}$ M can be described by the theoretical models for ac impedance of the so-called anomalous diffusion layer [I,82–85].

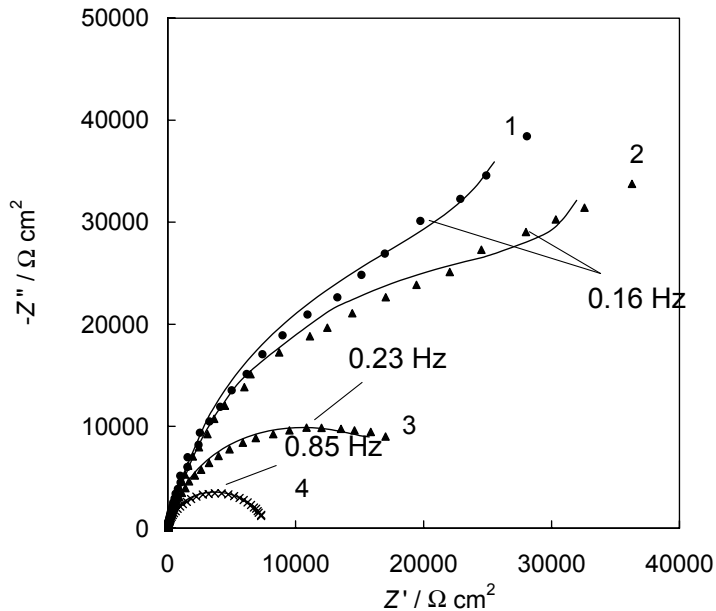


Fig. 5. Complex plane plots for the Bi(001) | 0.05 M Na₂SO₄ + 0.16mM SDS system at different electrode potentials, E (V / Ag | AgCl): -1.1 (1); -0.8 (2); -1.4 (3); and -1.5 (4) (points, experimental data; solid lines, calculated according to FMG; $\alpha_{\text{org}} = 0.5$).

The phase angle $|\delta|$, $\log f$ plots given in Fig. 6, demonstrate the complicated kinetic behaviour of Bi(*hkl*) | xM SDS+ 0.05M Na₂SO₄ interface. There are two maxima in $-\delta$, $\log f$ plots for $E > -1.2$ V and $c < 8 \times 10^{-4}$ M SDS solution indicating that there are two characteristic processes with very different characteristic time values as it was already observed in $-Z''$, Z' -plots. At more negative potentials, $E \ll E_{\max}$, the values of phase angle are decreasing caused by the slow Faraday processes.

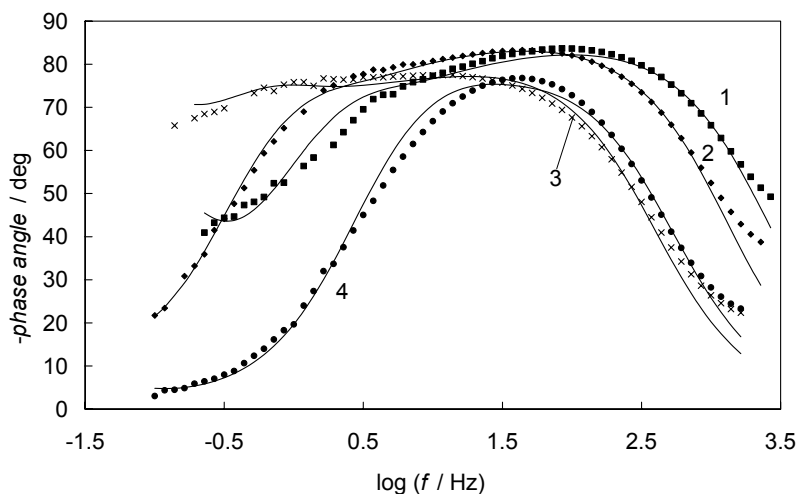


Fig. 6. Dependence of phase angle (δ) on ac frequency for Bi(001) in the aqueous 0.05 M Na₂SO₄ solution with addition of 0.4 mM SDS -0.8 V (1); -0.6 (2); -1.2 (3); and -1.6 (4) (marks- experimental data, lines- calculated according FMG).

The equilibrium differential capacitance curves (Fig. 7) have been established by the linear extrapolation of the $C_s, \omega^{1/2}$ curves to the condition $\omega^{1/2}=0$. In the region $-1.37 < E < -1.0$ V (Ag/AgCl), there are very nice adsorption-desorption peaks with the potential E^{peak} , depending parabolically on $\log c_{\text{SDS}}$ in good agreement with the Frumkin-Damaskin adsorption theory [VI,1,13,14]. Small additional steps in the C, E curves (at $E \geq -0.6$ V) for more concentrated SDS solution within the region of maximal adsorption, indicating the possibility of phase transitions in the adsorbed layer, have been observed for Bi(111) and Bi(001) planes [VI].

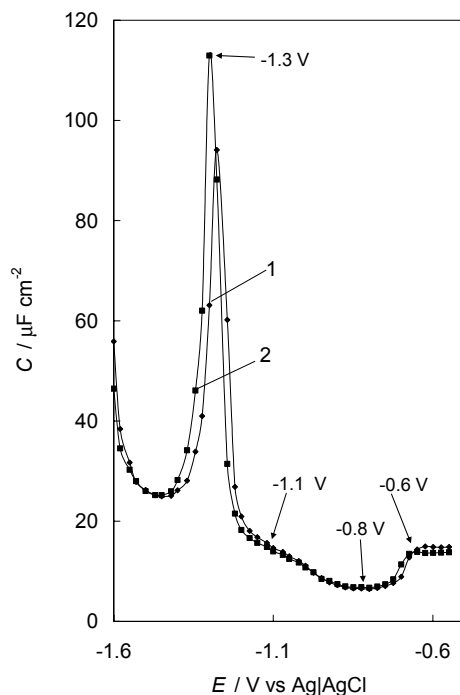


Fig. 7. Differential capacitance versus electrode potential curves (extrapolated to $f=0$ Hz) for Bi(001) | 0.05 M Na₂SO₄ + c M SDS system, for c_{SDS} , M: 1.6×10^{-3} (1); and 8×10^{-2} (2).

The data for $c_{\text{SDS}} < 1 \times 10^{-2}$ M (Fig. 7) show that the additional capacitance step at $-1.2\text{V} < E < -1.1\text{V}$ are clearly visible for Bi(111) and Bi(001) indicating to the hemi-micelle formation process at Bi(111) and (001) planes, similarly for Hg and Au(hkl) electrodes [92–94]. Very compact adsorption layer of SDS Bi(hkl) has been formed at $E=E_{\text{max}}$ [VI,64–66,70].

6.2.1. Calculation of the complex impedance plane plot parameters

Non-linear regression analysis of Z' , Z'' -curves for less concentrated SDS solutions $c_{\text{SDS}} \leq 3 \times 10^{-4}$ M show that for the first approximation at peak potentials the data can be simulated with the classical Frumkin-Melik-Gaikazyan (FMG) equivalent circuit presented in Fig. 1 (circuit b). The experimental data for more concentrated solutions ($c_{\text{SDS}} \geq 8 \times 10^{-4}$ M) in the region of maximal adsorption (at very low frequencies $f < 0.6$ Hz) can be simulated using the equivalent circuits (f) in Fig. 1 (i.e. by the Wandlowski- de Levie circuit), taking into account formation of compact adsorption layer at Bi(hkl).

The dependence of C_{true} and C_{ad} has minimal values in the region of zero charge potential (in the region of maximal adsorption) and increases quickly with desorption of the organic compound from the electrode surface with the rise of negative polarization of the electrode which is in a good agreement with the Frumkin-Damaskin adsorption theory of the neutral organic compound at the ideally polarizable electrode [I,VI,1,2,13,14].

The diffusion resistance R_D obtained at $\alpha_{\text{org}} = 0.5$ is maximal in the region of E_{max} . R_D increases with the increase of surface coverage and with decreasing the negative polarization of the Bi electrodes at fixed c_{SDS} .

6.2.2. Estimation of the limiting stage using classical analysis model

The Cole-Cole plots Fig. 8 have been calculated [VI]. The shape of Cole-Cole plots depends on the electrode potential and c_{SDS} . At $f > 1000$ Hz these dependences take the form of a slightly deformed quarter-circle, with the depression angle $\beta \leq 25^\circ$. Thus, in the region of higher frequencies ($1000 < f < 7000$ Hz), values of β somewhat lower than 45° , indicate of the mixed kinetics of the SDS adsorption at Bi planes (with $\tau_K^{\text{theor}} > \tau_D^{\text{theor}}$). At $E \approx E_{\text{max}}$, there is a practically linear dependence of $(\omega R_p)^{-1}$ on $(C_p - C_{\text{true}})$ (with the slope value $\beta' > 35^\circ$) at very low frequencies ($f < 5$ Hz), which is caused by the Warburg-like diffusion processes within the region of compact adsorption (surface) layer.

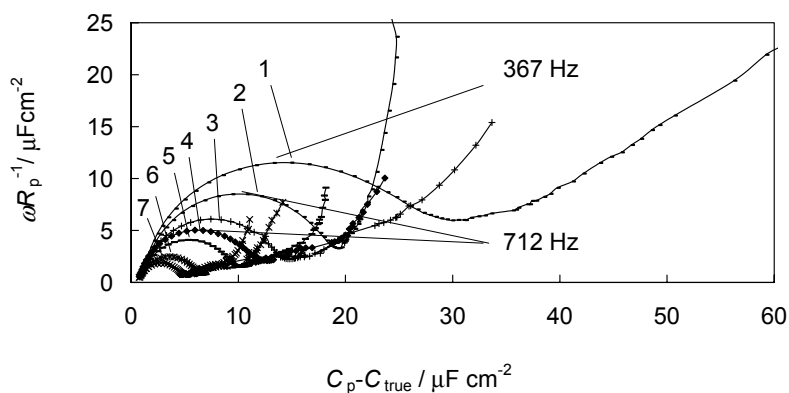


Fig. 8. Cole-Cole plots for Bi(111) plane in the 0.05 M $\text{Na}_2\text{SO}_4 + 8$ mM SDS solution at E (V vs. Ag|AgCl): -1.6 (1); -1.5 (2); -1.3 (3); -0.6 (4); -1.2 (5); -1.1 (6); -0.8 and (7).

The values of α_{exp}^* , calculated from the y^* , $\log f$ -dependence (Eq. 6.1.2.1) [1,11–13], indicate the mixed kinetics for adsorption of the SDS at Bi(111) and

Bi(001) planes. Only at $E=E_{\max}$ there are comparatively small deviation from diffusion limited process. The values of τ_{exp}^* (from y^* , $\log f$ -dependences) increase with c_{SDS} , being in a good agreement with the values of τ_{exp} obtained from Cole-Cole plots. τ_{exp} are maximal in the region of adsorption desorption peak potential as well as at $E=-1.1$ V where the additional step in C , E -curves (2D or 3D restructuring process) takes place.

The experimental $(\omega R_p)^{-1}$, $\log f$ -dependences have been simulated using Eqs (4.2.5, 4.2.10 and 4.2.14). According to the results of calculations, a better coincidence between of the experimental and calculated data was established when Eq. (4.2.14) (mixed kinetics with $\tau_k^{\text{theor}} \gg \tau_D^{\text{theor}}$) has been used [VI].

6.2.3. Thermodynamic adsorption parameters [VI]

The charge density values σ with addition of SDS in solution were obtained using back integration method starting from $E=-1.6$ V where the σ (with addition of organic molecules) and σ_0 (in base electrolyte) have been taken to be equal because there is no adsorption of SDS at $E=-1.6$ V (as the coincidence of C_0 and C_s values takes place) [1,2,13,14,89–91]. The data show that the maximal adsorption potential E_{\max} obtained from the potential of the concordance of σ_0 , E - and σ , E - curves is in good agreement with the E_{\max} values obtained from C_s , E -curves. Only for more concentrated $c_{\text{SDS}} \geq 1.6 \times 10^{-3}$ M E_{\max} values established using σ , E - curves are somewhat less negative than E_{\max} , obtained from C_s , E -curves. This surprising anomalous effect can be explained by the formation of more complicated adsorption layer structure (bilayer or probably 3-D adsorption or polylayers) than the monolayer of SDS at Bi(hkl) giving rise of σ values at $E=E_{\max}$ [92].

The σ , E -curves were back-integrated to obtain a specific surface work decrease as a function of E and adsorbate concentration [1,13,14]. The data shows that π values systematically increase with the rise of c_{SDS} and for more concentrated $c_{\text{SDS}} \geq 8 \times 10^{-3}$ M solutions the π values increase in the order of planes Bi(111) < Bi(01 $\bar{1}$) < Bi(001).

The values of Γ_{\max} obtained (Table 1) depend on Bi(hkl) studied and Γ_{\max} are higher for Bi(001) and lower Γ_{\max} values have been obtained for Bi(01 $\bar{1}$). Γ_{\max} for Bi(hkl) are slightly lower compared to the values of Γ_{\max} for Hg ($\Gamma_{\max}(\text{Hg}) = 3 \times 10^{-10}$ mol cm $^{-2}$) [III,92,94]. The values of the surface area occupied by one adsorbed molecule, S_{\max} (Table 1), are calculated from the values of Γ_{\max} and increase in the order of (001) < (01 $\bar{1}$) < (111) planes. The SDS molecules are probably oriented more perpendicularly at Bi(111) plane that for other planes.

The small shift of E_{\max} toward more negative electrode potential with the rise of c_{SDS} indicates to the increase of the positive E_N value, thus for the more vertical orientation of hydrocarbon chain or more expressed screening effect of negative charge of SDS anion by the base electrolyte Na^+ cations. The limiting E_N values obtained are given in Table 1.

The limiting differential capacitance data, presented in Table 1, show that the quite close values of C' for Bi(001) and Bi(111) planes as well as for Hg [92,93] have been obtained. The slope of $\log[\theta(1-\theta)c]$, θ -dependence gives the molecular interaction parameter ($-2a$), where the positive a values were obtained which indicates the strong interaction between SDS molecules. The a values are increasing in order $\text{Bi(111)} < \text{Bi(001)} < \text{Bi(01}\bar{1})$ as the electrochemical activity of plane increases.

The ΔG_{ads}^0 , E -curves display a parabolic behaviour (Fig. 9) in a good agreement with the Frumkin-Damaskin adsorption theory [7, 32, 33, 60]. The adsorption data of SDS in Table 1 show that the adsorption activity increases in the sequence of the electrodes $\text{Bi(001)} < \text{Bi(01}\bar{1}) < \text{Bi(111)} < \text{Hg}$ [92,93].

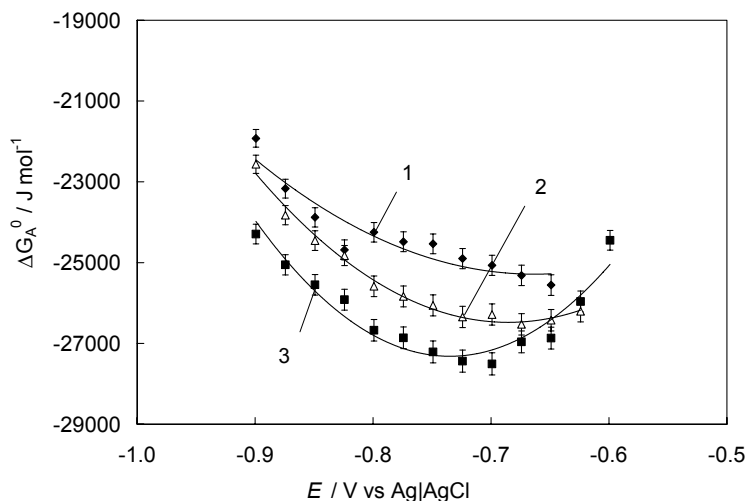


Fig. 9. Gibbs adsorption energy ΔG_A^0 , E - curves for SDS adsorption on Bi(001) (1), Bi(01 $\bar{1}$) (2), and Bi(111) (3).

6.3. Adsorption of camphor and 2, 2'-bipyridine on Bi(111)electrode surface [IV, V]

Impedance spectroscopy and *in situ* STM methods have been used for investigation of the camphor and 2,2'-bipyridine (2,2'-BP) adsorption at the electrochemically polished Bi(111) electrode from weakly acidified Na₂SO₄ supporting electrolyte aqueous solution.

Thus, according to systematic analysis, only the compounds having very compact adsorption layer, the formation kinetics of which is mainly limited by the rate of the heterogeneous adsorption step (like 2,2'-BP and camphor) can be visualized onto the Bi(111) surface by *in situ* STM method [IV], i.e. at $E \geq -0.6$ V in the case of 2,2'-BP and $E \geq -0.45$ V for camphor.

Analysis of the Nyquist (Fig. 10) and Bode phase angle vs. $\log f$ plots (Fig. 11) [V,1,2,11–21] shows that, in the region of *ac* frequency from 500 to 10 Hz, the camphor adsorption is limited mainly by the rate of the heterogeneous adsorption step and adsorption of 2,2' -BP is limited mainly by the mixed (slow heterogeneous adsorption and diffusion steps) kinetics because the phase angle values are lower than -75° [V] like uracil adsorption on Bi(*hkl*) [I].

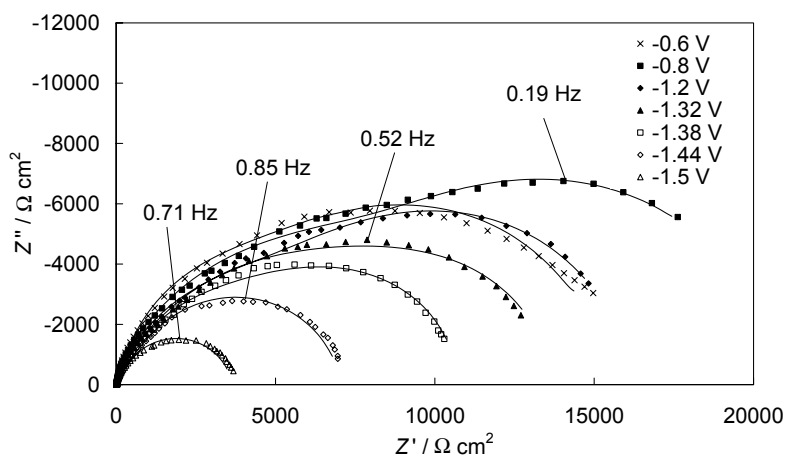


Fig. 10. Nyquist plots for Bi(111) in the supporting electrolyte (5×10^{-2} M Na₂SO₄) + 5×10^{-3} M camphor solution at various electrode potentials (v vs. Ag|AgCl, noted in figure).

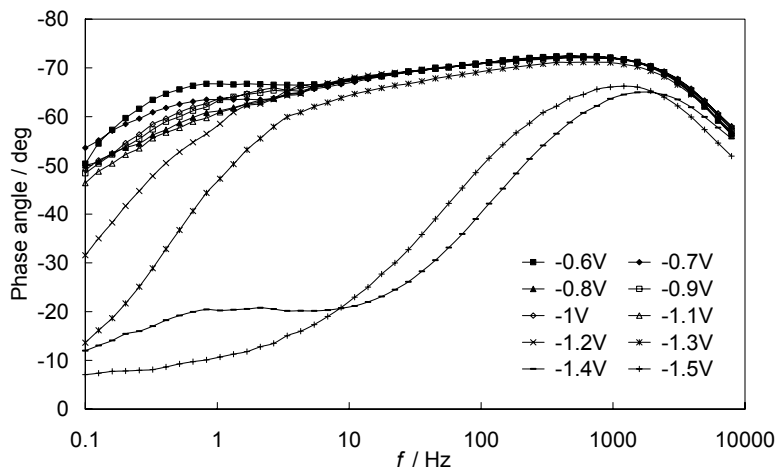


Fig. 11. Bode plots for various electrode potentials (V vs. Ag|AgCl, noted in figure) at Bi(111) plane in supporting electrolyte (0.05M Na₂SO₄) + 0.003M 2, 2'-bipyridine solution.

The characteristic relaxation time $\tau_m = (2\pi f_m)^{-1}$ obtained from Nyquist plots varies from 0.7 s (at $E = -1.2$ V) to 0.43 s (at $E = -0.80$ V) for camphor and τ_m is over 0.3 s for 2,2'-BP at $E = -1.3$ V. However, at $E > -1.3$ V it is not possible to obtain τ_m values because of the very slow adsorption kinetics of 2,2'-BP. The same conclusion can be made according to the classical analysis method based on the Cole-Cole plots [11–14] and Lorenz analysis method [16,23]. Comparison of the data in Cole-Cole plots shows that the total resistance of adsorption process increases with c_{camphor} and $c_{2,2'\text{-BP}}$ in the supporting electrolyte solution at $E = E_{\text{max}}$. It should be noted that for the formation process of a real 2D condensation layer there would be an exponential dependence of τ_m on E [95–107]. The noticeably less expressed dependence of τ_m on E probably indicates that there is no classical 2D condensation of the camphor molecules on the Bi(111) electrode surface at $T = 298$ K.

The systematic analysis of Nyquist plots (Fig. 10) shows that in the region of maximum adsorption the experimental data, to a first very rough approximation, can be fitted by the classical Frumkin Melik-Gaikazyan equivalent circuit (circuit b in Fig. 1), which takes into account only the semi-infinite diffusion and heterogeneous adsorption limited steps [IV,V,1,11, 13,14].

However, a better fit has been observed if the Wandlowski – de Levie equivalent circuit [78–80], taking into account the two-dimensional association of the molecules adsorbed in the adsorption layer, has been used (circuit f in Fig. 1). The parameters from the Wandlowski-de Levie model depend on the electrode potential as well as on the concentration of organic compound being

in good agreement with the theory of the adsorption of organic compounds on the ideally polarizable electrodes [1,13,14].

In the region of maximal adsorption, i.e. in the region of capacitance pit in the differential capacitance vs. electrode potential curve the main rate determining stages are the heterogeneous adsorption step for camphor and slow heterogeneous adsorption and diffusion steps (mixed kinetics) for 2,2'-BP adsorption on the electrochemically polished Bi(111) electrode, but not only the classical semi-infinite diffusion step as usually assumed [I,IV,V].

For 2,2'-BP | Bi(111) interface the adsorption layer structure is very well detectable by *in situ* STM technique (Fig. 12) in the region of maximal adsorption (i.e. near zero charge potential) from -0.6 V to -0.4 V vs. Ag/AgCl). This is mainly caused by the comparatively strong interaction of nitrogen atoms of 2,2'-BP (electron pairs at nitrogen) with Bi surface layer atoms and high negative Gibbs adsorption energy values ($\Delta G_A^0 = -29.8$ kJ mol $^{-1}$) obtained using Frumkin adsorption isotherm data [1,13,14,86,87,89,90]. It was found that camphor adsorption adlayer is detectable only at positive surface charge densities, where the co-adsorption of SO_4^{2-} takes place. This can be explained by the less negative ($\Delta G_A^0 = -21.1$ kJ mol $^{-1}$) values for camphor in comparison with Bi(111) | 2,2'-BP + 0.5M Na_2SO_4 interface.

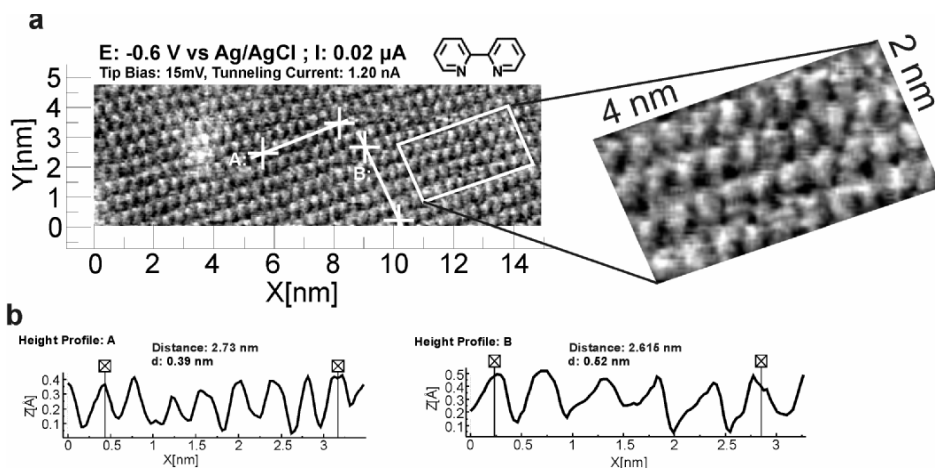


Fig. 12. Unfiltered *in situ* STM image and selected 8nm 2 section with 40 2, 2'-bipyridine molecules (a) and selected height profile (b) from 2, 2'-bipyridine adlayer on Bi(111) electrode surface in 25×10^{-2} M 2, 2'-bipyridine + 0.5M Na_2SO_4 + 3×10^{-3} M H_2SO_4 aqueous electrolyte.

The corresponding values of $\Delta G_{\text{int}}^0 = -2aRT = -9.46$ kJ mol $^{-1}$ for camphor and -6.9 kJ mol $^{-1}$ for 2,2'-BP indicate that the van der Waals interaction for camphor molecules is even higher than for 2,2'-BP adsorption on Bi(111), but

the Gibbs adsorption free energy is noticeably lower for camphor in comparison with 2,2'-BP. The values of Gibbs adsorption ΔG_A^0 for 2,2'-BP and camphor at Bi(111) calculated from *in situ* STM data ($\Gamma_{\max} = 8.3 \times 10^{-10} \text{ mol cm}^{-2}$, $\Gamma_{\max} = 3.4 \times 10^{-10} \text{ mol cm}^{-2}$ respectively) are in a very good agreement with those obtained from impedance spectroscopy data [IV,V].

6.4. Comparison of some adsorption kinetic and thermodynamic parameters of uracil, tetrabutylammonium cations, sodium dodecyl sulfate, camphor and 2, 2'-bipyridin on Bi single crystal plane

6.4.1. Analysis of Nyquist plots

The systematic analysis of Nyquist plots shows that in the region of $-1.6\text{V} < E < -0.6\text{V}$ and for dilute solutions the experimental data, to a first very rough approximation, can be fitted by the classical Frumkin- Melik-Gaikazyan equivalent circuit (circuit b in Fig. 1) [32–33,43], which takes into account the adsorption and diffusion limited steps [I,II,V,VI,1,11,13,14]. The replacement of Warburg-like diffusion impedance by the partial charge transfer resistance R_{ad} ; so-called Dolin-Ershler circuit [108]) did not give a better fit of the experimental with the calculated data. Only a very slightly better fit of the experimental data (mainly at $E > -1.3\text{V}$ and for less concentrated solutions) in the case of uracil and TBA^+ adsorption was established if the constant phase element CPE_1 instead of C_{true} was introduced into Frumkin-Melik-Gaikazian circuit (Fig. 1 circuit c) [I, II]. However, the χ^2 -function and weighted sum of squares were in same range and therefore the modified Frumkin-Melik-Gaikazian circuit was not justified totally. The attempt to add the additional elements into these equivalent circuits did not give a better fit of experimental data. Therefore for less concentrated uracil, TBA^+ , SDS, camphor and 2, 2'-BP at $E < -1.3\text{V}$, the classical Frumkin-Melik-Gaikazian circuit [9] (to a first approximation) seems to be a more probable physical model as it is the simplest circuit, giving a better fit to experimental results [1,13,14].

The experimental data for more concentrated solutions in the region of maximal adsorption (at very low frequencies $f < 0.6 \text{ Hz}$) can be simulated using the Wandlowski- de Levie circuit (Fig. 1 circuit e), taking into account formation of compact adsorption layer at $\text{Bi}(hkl)$ [I, II, IV, V, VI].

At more negative electrode potentials (in the region from -1.3 to -1.5 V) and concentrated solutions there are some deviation from the Wandlowski-de Levie circuit, where the slow faradaic hydrogen evolution starts. Therefore in the region $E < -1.3\text{V}$ in the system $\text{Bi}(hkl)| \text{SDS}^+ \text{ base electrolyte}$ interface the

circuit (g) in Fig. 1, where the charge transfer resistance R_{ct} is added in parallel to the adsorption branch, can be used [I,VI].

The values of diffusion resistance R_D , obtained according to FMG ($\alpha=0.5$) model for uracil and SDS and according to Wandlowski de Levie model for TBA⁺ camphor and 2, 2'-BP are maximal in the region of maximal adsorption. The high values of R_D indicate that the compact adsorption layer has been formed at the Bi(*hkl*) surface at $E = E_{max}$. R_D quickly decreases with the negative surface charge density. R_D has small maxima at $E=E^{peak}$ for dilute organic compound solutions [V,VI], when the adsorption-desorption maxima are in the development stage (ie at $\theta \approx 0.5$). The same effect was found for uracil and tetrabutylammonium cation adsorption [I, II]. R_D values depend on the crystallographic structure of Bi planes studied and R_D values are minimal for most active Bi(01 $\bar{1}$) plane and highest for Bi(111).

The adsorption capacitance C_{ad} values are minimal at the potential of maximal adsorption in good agreement with the Frumkin-Damaskin adsorption theory for neutral organic compounds at ideally polarizable electrodes [1,13,14]. C_{ad} values at $E=E_{max}$ are nearly independent of Bi(*hkl*) plane studied. The very high values of C_{ad} have been established for more concentrated uracil solutions at electrode potentials more negative than $E < -1.3V$, indicating that the peaks are influenced by the faradaic pseudo-capacitance (slow hydrogen evolution reaction) or by the partial charge transfer process.

Dependence of C_{true} on the electrode potential at $E > -1.3 V$ is in a good agreement with the Frumkin-Damaskin adsorption theory of the organic compound at the ideally polarizable electrode [I,II,III,IV,V,VI]. C_{true} has minimal values in the region of zero charge potential (in the region of maximal adsorption) and increases quickly with desorption of the organic compound from the electrode surface with the rise of negative polarization of the electrode.

The needle peak capacitance C_n and needle peak resistance R_n were obtained using Wandlowski de Levie model [II,IV,V,VI]. The needle peak capacitance C_n is low in the region of adsorption-desorption peaks and the rise of C_n at $E < E^{peak}$ is mainly caused by the parallel hydrogen evolution reaction at the electrode surface areas free from adsorbed organic molecules [II,IV,V,VI]. The needle peak resistance R_n depends on the concentration of organic molecules and electrode potential, and R_n is low in the region of adsorption-desorption peaks like for the tetrabutylammonium cations adsorption on Bi(01 $\bar{1}$) and for camphor and 2,2'-BP adsorption on Bi(111) [II, IV].

6.4.2. Estimation of the limiting stage

The Cole-Cole plots take the form of a slightly deformed quarter-circle at $f > 1000$ Hz, with the depression angle $\beta \leq 25^\circ$ in the case of uracil and SDS. Thus, in the region of higher frequencies ($1000 < f < 7000$ Hz), the values of β

somewhat lower than 45° , indicate mixed kinetics of the SDS and uracil adsorption at Bi planes with $\tau_K > \tau_D$ [I, VI]. In the case of diffusion limitation the Cole-Cole plots take the form of a quarter – circle with the depression angle values of $\beta = 45^\circ$, this can be seen in the Bi(*hkl*)|base electrolyte+ TBA⁺ and camphor system at higher frequencies ($f > 1000$ Hz) [II, IV]. In the region of small frequencies ($1.0 < f < 100$ Hz) the values of the depression angle β' are noticeably higher ($\beta' \geq 40^\circ$) than those at $f > 1000$ Hz and indicate that, in the region of moderate ac frequencies, the deviation from the diffusion limitation is smaller as for *ac* frequencies $f > 1000$ Hz, the $1/\omega R_p, C_p$ -dependence can be simulated by a quarter-circle with the centre lying lower than the C_p -axis [I, II, V]. The values of experimental relaxation time $\tau_{\text{exp}} = (\omega_{\text{max}})^{-1}$, are somewhat higher for the more concentrated solutions and this is probably mainly caused by the formation of the compact adsorption layer at Bi(*hkl*) and obtained τ_{exp} values depend noticeably on the electrode potential, and the values of τ_{exp} increase with a decrease of negative electrode potential, i.e. with an increase of compactness of the adsorption layer [I, VI]. Comparison data for uracil, SDS and TBA⁺ [I, II, V] demonstrates comparatively quick mainly diffusion-limited process of TBN⁺ cations. However, as for uracil and dodecyl sulfate anion adsorption at $E = E_{\text{max}}$, there are noticeable deviations from the semicircle at lower ac frequency ($f < 50$ Hz), which can be explained by the diffusion-like process in the adsorption layer (formation of two-dimensionally ordered areas or restructuring of the adsorption layer) as in this region of the Cole-Cole plots, the linear dependence of $(\omega R_p)^{-1}$ on C_p with the slope value $\beta'' \sim 45^\circ$ has been established. The values of τ_{exp} depend somewhat on the crystallographic structure of the electrode, and τ_{exp} decreases with the increase of Frumkin attraction coefficient a from Bi($01\bar{1}$) to Bi(111) [I,II,V,VI].

The experimental $(\omega R_p)^{-1}, \log f$ -dependences have been simulated using Eqs (4.2.4–4.2.14). According to the results of calculations a better fit between the experimental and calculated data was established when Eq. (4.2.14) characteristic mixed kinetic process has been used. The values of τ_D^{theor} and τ_K^{theor} in the case of uracil and SDS indicate that the adsorption process is limited mainly by the heterogeneous adsorption step as values of τ_D^{theor} smaller than τ_K^{theor} were established [I, VI]. The values of τ_D^{theor} and τ_K^{theor} depend somewhat on the concentration in solution. However, the values of τ_K^{theor} practically coincide with the experimental values of τ_{exp} and therefore, to a first approximation, the values of τ_{exp} at $f > 40$ Hz characterize the relaxation time of the heterogeneous adsorption step. However, there are noticeable differences between the experimental and calculated $(\omega R_p)^{-1}$ values at the small ac frequency values ($f < 10$ Hz) [I, V]. Differently from uracil and SDS the τ_D^{theor} values for TBA⁺ are much higher than τ_K^{theor} and indicate that diffusion is the main rate- determining step for TBA⁺ adsorption at Bi($01\bar{1}$) plane [II].

6.4.3. Thermodynamic adsorption parameters

The differential capacitance vs. electrode potential curves were measured for all systems studied. For uracil and SDS at Bi(*hkl*) the equilibrium capacitance C versus E -curves have been obtained by the linear extrapolation of the $C_s, \omega^{1/2}$ -curves [III, V] to the condition $\omega^{1/2}=0$. Differently from Bi(*hkl*)|SDS, camphor, TBA⁺ and 2,2'-BP in the case of uracil there is no very well developed adsorption-desorption peak in C, E -curves at more negative potentials and C only start to increase with the negative polarization of the electrode. At more positive electrode potentials the capacitance starts to decrease to a value much smaller than that observed for the base electrolyte. For camphor, SDS, 2, 2'-BP and TBA⁺ the stable physical adsorption layer is very well detectable. At more negative potential than $E=E_{\max}$ the reorientation peaks were detectable in differential capacitance vs. electrode potential curves for uracil and SDS only [III,VI]. However, small additional step in C, E -curves for TBA⁺ adsorption at Bi(01 $\bar{1}$) electrode were obtained.

The limiting capacitance values C' were obtained and are given in Table 1. The C' values are lowest in the case of 2, 2'-BP where the very well ordered two-dimensional adsorption layer is detectable by the in situ STM method [IV,V].

For Bi(*hkl*)|SDS system the small shift of E_{\max} toward more negative electrode potential with the rise of c_{SDS} indicates to the increase of the positive E_N value, thus for the more vertical orientation of SDS hydrocarbon chain or more expressed screening effect of negative charge of SDS anion by the Na⁺ cations [VI]. Differently from SDS [VI] the negative values of E_N were calculated for uracil [III] adsorption and this indicates that the uracil molecules are oriented with the negative dipole end toward the Bi(*hkl*) surface.

The projected area S_{\max} decreases and Γ_{\max} (Table 1) increases in the order TBA⁺<SDS < uracil < camphor < 2,2'-BP, which can be explained by the increase of packing density of an organic compound in adsorption monolayer (I-VI).

The applicability of Frumkin isotherm was tested using the $\log[\theta/(1-\theta)c], \theta$ -plot method and it can be seen in the papers [II, V] that these plots have good linearity and the Frumkin model [1,13,14] seems to be valid. The slope of the Frumkin isotherm gives the interaction parameter ($-2a$). The a values (Table 1) are highest for camphor and comparable results have been calculated for uracil and 2,2'-BP, relatively low a values were obtained for sodium dodecyl sulfate adsorption (Table 1) at Bi(*hkl*) interface.

The energetics of SDS, uracil, camphor and 2, 2'-bipyridin adsorption was characterized by the magnitude of the Gibbs energy of adsorption $\Delta G_{\text{ads}}^0 = -RT \ln(55.5B)$ (Table 1). The adsorption data for SDS in Table 1 show that the adsorption activity increases in the sequence of the electrodes Bi(001) < Bi(01 $\bar{1}$) < Bi(111) [VI] in the case of uracil adsorption Bi(111) < Bi(01 $\bar{1}$) [I].

According to the data in Table 1. the adsorption activity of adsorbate rises in the sequence uracil<camphor<SDS<2, 2'-BP. The value of ΔG_{ads}^0 for 2, 2'-BP is noticeable lower compared with the other system studied Bi(*hkl*) indicating to the noticeable more strong adsorption of 2, 2'-BP at Bi(*hkl*) compared with others compound studied.

The obtained negative values of $-\Delta G_{int}^0$ and the positive values of *a* mean that the interactions between adsorbed molecules (A-A and W-W) are more attractive than the adsorbate-water interactions [III,IV,V,VI]. In accordance with the experimental data values of $-\Delta G_{int}^0$ are given in Table1 [1-6]. $-\Delta G_{int}^0$ indicates that the van der Waals interaction are higher for camphor as well as for 2, 2'-BP and uracil molecules, but the comparatively less negative values of $-\Delta G_{int}^0$ were obtained for SDS adsorption, explained with the not totally screened charged effect of an anion by Na⁺ cation in the compact adsorption layer.

7. SUMMARY

Electrochemical behaviour of uracil, tetrabutylammonium cations (TBA^+), sodium dodecyl sulfate (SDS), camphor and 2, 2'-bipyridin (2, 2'-BP) on the electrochemically polished Bi single crystal planes in 0.05 M Na_2SO_4 aqueous solution has been studied by electrochemical impedance and *in situ* STM method. The thermodynamic adsorption parameters and the adsorption kinetics including mechanisms and limiting steps has been obtained and analysed.

The complex impedance plane plots were simulated using different equivalent circuits, like Frumkin-Melik-Gaikazyan, modified Frumkin-Melik-Gaikazyan, Wandlowski -de Levie and other models.

To the first approximation the impedance data obtained for the systems investigated can be simulated in diluted adsorbate solutions by the classical Frumkin-Melik-Gaikazyan model. For concentrated solutions more complicated models has been used. In the region of maximal adsorption potential $E=E_{\text{max}}$ Wandlowski- de Levie model taking into account the two-dimensional condensation process seems to be more appropriate.

According to the non-linear least-square fitting data, C_{true} , C_{ad} and C_n have minimal values in the region of maximal adsorption and increase quickly with desorption of the organic compound from the electrode surface and with the rise of negative polarization of the electrode. The parameters R_D and R_N have maximal values in the region of maximal adsorption. The high values R_D and R_N indicate that the compact adsorption layer has been formed at the Bi(*hkl*) surface at $E = E_{\text{max}}$. R_D and R_N are quickly decreasing with the negative surface charge density.

Systematic analysis of the frequency related admittance i.e. Cole-Cole dependences shows that in the region $E=E_{\text{max}}$ the main rate determining stage are the heterogeneous adsorption step for camphor and slow heterogeneous adsorption and diffusion step (mixed kinetics) for 2, 2'-BP, SDS and uracil at Bi planes studied. In the case of TBA^+ there is only small deviation of system from the diffusion limited kinetics.

The C' values are smallest in the case of 2, 2'-BP where the very compact two-dimensional adsorption layer is very well detectable by the *in situ* STM and impedance methods [IV] has been formed.

Frumkin adsorption isotherms for the adsorption of uracil, TBA^+ and SDS on the Bi planes are practically linear within the region of surface coverage $0.1 < \theta < 0.8$. The positive values of the molecular interaction parameter a and negative values of Gibbs interaction energy in the adsorption layer means that the surfactant-surfactant and the water-water interactions are much more attractive than the surfactant-water interaction.

The projected area S_{max} decreases and Γ_{max} increases in the order of adsorbates $\text{TBA}^+ < \text{SDS} < \text{uracil} < \text{camphor} < 2,2'\text{-BP}$, which can be explained

by the increase of packing density of an organic compound in an adsorbed monolayer.

The negative Gibbs adsorption energy increases in the order of adsorbates: uracil < camphor < SDS < 2,2'-BP indicating to the increase of adsorption activity of adsorbates at Bi(*hkl*) in the presented order.

8. REFERENCES

- [1] B.B. Damaskin, O.A. Petrii, V.V. Batrakov, Adsorption of Organic Compounds on Electrodes, Plenum Press, New York, 1971, p.35.
- [2] G.Nurk, A.Jänes, K.Lust, E.Lust, J.Electroanal. Chem, 515 (2001) 17.
- [3] A.N. Frumkin, V.I. Melik-Gaikazyan, Dokl. Akad. Nauk USSR 77, (1951) 885.
- [4] V. Brabec, S. D. Christian, G. Dryhurst, Biophys. Chem. 7 (1978) 253.
- [5] G. Nurk, A. Jänes, P. Miidla, K. Lust, E. Lust, J. Electroanal. Chem. 515 (2001) 33.
- [6] E. Lust, A. Jänes, K. Lust, J. Ehrlich, Electrochimica Acta 44 (1999) 4707.
- [7] A. N. Frumkin, Potentsialy Nulevogo Zaryada (Potentials of Zero Charge), Nauka, Moscow, 1979, pp.153–176.
- [8] A. N. Frumkin, Z. Phys. Chem. 116 (1925) 446.
- [9] V.I. Melik-Gaikazyan, Zh. Fiz. Khim. 26 (1952) 560.
- [10] M. Sluyters-Rehbach, J. Sluyters, in: A. Bard (Ed.), Electroanalytical Chemistry, Vol. 4, Marcel Dekker, New York, 1970, p. 76.
- [11] R.D. Armstrong, W.P. Rice, H.R. Thirsk, J. Electroanal. Chem. 16 (1968) 517.
- [12] K.S. Cole, R.H. Cole, J. Chem. Phys. 9 (1941) 341.
- [13] A.N. Frumkin, B.B. Damaskin, in: J.O'M. Bockris, B.E. Conway (Eds.), Modern Aspects of Electrochemistry, vol. 3, 1964, p. 149.
- [14] B.B. Damaskin, L.N. Nekrassov, O.A. Petrii, B.I. Podlovchenko, E.V. Stenina, N.V. Fedorovich, in: B.B. Damaskin (Ed.), Electrochemical Properties in Organic Compound Solutions, Moscow University Press, Moscow, 1985, pp. 80–85 (in Russian).
- [15] U. Retter, H. Jering, J. Electroanal. Chem. 46 (1973) 375.
- [16] W. Lorenz, F. Möckel, Z. Elektrochem. 60 (1956) 507.
- [17] T.J. VanderNoot, J. Electroanal. Chem. 300 (1991) 199.
- [18] G.A. Tedoradze, R.A. Arakelyan, Dokl. Akad. Nauk SSSR 156 (1964) 1170.
- [19] E.J. Lust, U.V. Palm, Sov. Electrochem. Engl. Transl. 24 (1988) 227.
- [20] [A. Jänes, G. Nurk, K. Lust, E. Lust, Russ. J. Electrochem. 38 (2002) 11.
- [21] A. Jänes, E. Lust, Electrochimica Acta, 47 (2001) 967.
- [22] S. Trasatti, E.Lust, O. M. Bocris, R. E. White, B.E. Conway (Eds.) Modern Aspects of Electrochemisry, Vol. 33, Kluwer Academic/ Plenum Publishers, New York, 1999, pp. 1–216.
- [23] W. Lorenz, Z. Elektrochem. 62 (1958) 192.
- [24] A. Zangwill, Physics at Surfaces, Cambridge University Press, Cambridge, 1988.
- [25] E. Budevski, G. Saikov, W. J. Lorenz, Electrochemical Phase Phormation and Growth, VCH, Weinheim, 1996.
- [26] C. Buess-Herman, S. Bare, M. Poelman et al., in Interfacial Electrochemistry (Ed.:A. Wieckowski), Marcel Dekker, New York, 1999, pp. 427–452.
- [27] A Wieckowski, Interfacial Electrochemistry, Markel Dekker, New York, 1999.
- [28] J. A. Venable, Introduction to Surface and Thin Film Processes, Cambridge University Press, Cambridge, 2000.
- [29] W.J. Lorenz, W. Plieth, Electrochemical Nanotechnology, Wiley/VCH, Weinheim, 1998.
- [30] J. Lipkowski, P. N. Ross, Adsorption of Organic Molecules at Metal Electrodes, VCH, New York, 1992.

- [31] D. M. Kolb, *Prog. Surf. Sci.*, 51(1996) 109–173.
- [32] H. S. Nalwa, *Handbook of Nanostructured Materials*, Academic Press, San Diego, 2000, Vol.5.
- [33] G. A. Somorjai, *Introduction to Surface Chemistry and Catalysis*, John Wiley&Sons, New York, 1994.
- [34] A. Beiker, J. D. Grunwaldt, Ch. A. Müller et al., *Chimia*, 52(1998) 517–524.
- [35] A. Ahmadi, G. Attard, J. Feliu et al., *Langmuir*, 15(1999) 2420–2424.
- [36] N. J. Tao, *Phys. Rev. Lett.*, 76(1996) 4066–4069.
- [37] C. Buess-Herman, *Prog. Surf. Sci.*, 46(1994) 335–375.
- [38] T. Hill, *Statistical Mechanics*, McGraw Hill, New York, 1956, pp.286–353, Chap.7.
- [39] T. Hill, *Statistical Thermodynamics*, Addison Wesley, Reading, 1962.
- [40] W. Bragg, E. Williams, *Proc. R. Soc.London, Ser.*, 145 (A 1934) 699–730.
- [41] W. Bragg, E. Williams, *Proc. R. Soc.London, Ser.* 151(A 1935) 540–566.
- [42] R. Fowler, E.Guggenheim, *Statistical Thermodynamics*; Cambridge University Press, London, 1939.
- [43] P. Delahay, I. Trachtenberg, *J. Am. Chem. Soc.*, 79 (1957) 1362–2355.
- [44] R. Srinivasan, R. de Levie, *J. Electroanal. Chem.*, 205 (1986) 303–307.
- [45] P. Delahay, D. Mohilner, *J. Am. Chem. Soc.*, 84(1962) 4247–4252.
- [46] J. Michailik, B. B. Damaskin, *Sov. Electrochem.*, 15(1979)478–481.
- [47] N. Emanuel, D. Knorre, *Kurs Chimitschesoi Kinetiki*; Wyschaja schkola, Moskwa, 1962.
- [48] N. J. Tao, in *Imaginar of Surface and Interfaces* (Eds.: J. Lipkowski, P. N. Ross), John Wiley&Sons, New York, 1999, pp. 211–248.
- [49] B. Roelfs, E. Bunge, CSchröter et al., *J. Phys. Chem.*, 101(B 1997) 754–765.
- [50] Th. Dretschkow, Th Wandlowski, *Electrochim. Acta*, 43 (1998) 2843–2856.
- [51] F. Cunha, N. J. Tao, *Phys. Rev. Lett.*, 75 (1995) 2376–2379.
- [52] F. Cunha, Q. Jing, N. J. Tao, *Surf. Sci.*, 389 (1997) 19–28
- [53] J. Pan, S. M. Lindsay, N. J. Tao, *Langmuir*, 9(1993) 1556–1560.
- [54] N. J. Tao, Z. Shi, *J. Phys. Chem.*, 98 (1994) 7422–7426.
- [55] Cl. Buess-Herman, L. Gierst, N. Vanlaethem-meuree, *J. Electroanal. Chem.*, 123(1981)1–19.
- [56] Th. Wandlowski, G. B. Jameson, R. de Levie, *J. Phys. Chem.*, 97(1993) 10119–10126.
- [57] Th. Wandlowski, R. de Levie, *J. Electroanal. Chem.*, 329(1992)103–127.
- [58] R. Guidelli, M. L. Foresti, *J. Electroanal. Chem.*, 197 (1986) 123–141.
- [59] Th. Wandlowski, P. Chaiyasith, H. Baumgärtel, *J. Electroanal. Chem.*, 346(1992)271–279.
- [60] B. B. Damaskin, N. K. Akhmetov, *Sov. Electrochem.*, 15(1979) 478–481.
- [61] Yu. Kharkats, *J. Electroanal. Chem.* 115(1980)75–88.
- [62] Yu. Ya. Gurevich, Yu. I. Kharkats, *J. Electroanal. Chem.*, 86 (1978) 245–258.
- [63] U. Retter, H. Lohses, *J. Electroanal. Chem.*, 134 (1982) 243–250.
- [64] P. Niklitas, *J. Electroanal. Chem.*, 300(1991) 607–628.
- [65] P. Nikitas, *Electrochim.Acta*, 36(1991) 447–457.
- [66] P. Nikitas, S. Andoniou, *J. Electroanal. Chem.*, 375 (1994) 339–356.
- [67] U. Retter, *J. Electroanal. Chem.*, 165 (1985)221–230.
- [68] U. Retter, *J. Electroanal. Chem.*, 41 (1996) 41–48.
- [69] R. Sridharan, R. de Levie, *J. Phys. Chem.*, 86 (1982)4489, 4490.

- [70] G. Nurk, H. Kasuk, K. Lust, A. Jänes, E. Lust, *J. Electroanal. Chem.* 553 (2003) 1.
- [71] G. Brug, A. van der Eeden, M. Sluyters-Rehbach, J. Sluyters, *J. Electroanal. Chem.* 176 (1984) 275.
- [72] J.R. MacDonald (Ed.) *Impedance Spectroscopy: Emphasizing Solid Materials and Systems*, John Wiley & Sons, New York, 1987.
- [73] B.A. Boukamp, *Equivalent Circuit User's Manual*, University of Twente, 1989.
- [74] B.A. Boukamp, *J. Electrochem. Soc.* 142 (1995) 1885.
- [75] ZView for Windows (version 2.2) fitting program, Scribner Inc., Souther Pines, NC, 1999
- [76] M. Sluyters-Rehbach, *Pure and Appl. Chem.* 66 (1994) 1831.
- [77] A. Lasia, in B.E. Conway, J.O'M. Bockris, R.E. White (Eds.), *Modern Aspects of Electrochem.*, Vol. 32, Plenum Press, New York, 1999, pp. 143–248.
- [78] T. Wandlowski, R. de Levie, *J. Electroanal. Chem.* 345 (1993) 413.
- [79] T. Wandlowski, R. de Levie, *J. Electroanal. Chem.* 352 (1993) 279.
- [80] T. Wandlowski, R. de Levie, *J. Electroanal. Chem.* 380 (1995) 201.
- [81] A. Jänes, K. Lust, E. Lust, *J. Electroanal. Chem.* 548 (2003) 27.
- [82] T. Jakobsen, K. West, *Electrochim. Acta*, 40 (1995) 233.
- [83] A. Compte, R. Netzlek, *J. Phys. A.: Math. Gen.* 30 (1997) 7277.
- [84] J. Bisquert, G. Garcia-Belmonte, P.R. Bueno, E. Longo, L.O. S. Bulhøoe, *J. Electroanal. Chem.*, 452(1998) 229
- [85] A. Bisquert, A. Compte, *J. Electroanal. Chem.*, 499 (2001) 112.
- [86] E.J. Lust, K.K. Lust and A.A.-J. Jänes. *Russ. J. Electrochem.* 31 (1995), p. 876.
- [87] E. Lust, K. Lust and A. Jänes. *J. Electroanal. Chem.* 413 (1996), p. 111.
- [88] T. Pajkossy. *J. Electroanal. Chem.* 364 (1994), p. 111.
- [89] E. Lust, A. Jänes, K. Lust, R. Pullerits, *J. Electroanal. Chem.* 431 (1997) 183.
- [90] E. Lust, A.J. Bard, M. Stratmann (Eds.), *Encyclopaedia of Electrochemistry*, Vol.1, VCH-Wiley, Weinheim, 2000.
- [91] V. Brabec, S.D. Christian, G. Dryhust, *J. Electroanal. Chem.* 85 (1977) 389.
- [92] B. B. Damaskin, N. N. Nikolayeva-Fedorovich, R.V. Ivonova, *Zh. Fiz. Khim.*, 34(1960)899.
- [93] T. Wandlowski, M. Hromodova, R. de Levie, *J. Electroanal Chem.*, 324 (1992) 375.
- [94] I. Burgess, C.A. Jettzey, X. Cai., G. Szykanski, Z. Galus, J. Lipkowski, *Langmuir*, 15(1999)2607.
- [95] Th. Wandlowski, K. Ataka, D. Mayer, *J. Electroanal. Chem.*, 524(2002)20.
- [96] Th. Wandlowski, E. Kretschmer, E. Müller, F. Kuschel, S. Hoffmann, K. Janta von Lipinski, *J. Electroanal. Chem.*, 7 (1978) 253.
- [97] R. de Levie and Th. Wandlowski. *J. Electroanal. Chem.* 366 (1994), p. 256.
- [98] M.H. Hölzle, D. Kranich and D.M. Kolb. *J. Electroanal. Chem.* 386 (1995), p. 235.
- [99] M.H. Hölzle, Th. Wandlowski and D.M. Kolb. *Surf. Sci.* 335 (1995), p. 281.
- [100] S. Bare and C. Buess-Herman. *Colloids Surf. A: Physicochem. Eng. Aspects* 134 (1998), p. 181.
- [101] Th. Wandlowski and M.H. Hölzle. *Langmuir* 12 (1996), p. 6604.
- [102] F. Heiglein, D.M. Kolb and J. Lipkowski. *Surf. Sci.* 291 (1993), p. 325.
- [103] U.W. Hamm and D.M. Kolb. *J. Electroanal. Chem.* 332 (1992), p. 339.

- [104] B.M. Ocko, O.M. Magnussen, R.R. Adzic, J. Wang, Z. Shi and J. Lipkowski. *J. Electroanal. Chem.* 376 (1994), p. 1384.
- [105] Th. Wandlowski, B.M. Ocko, O.M. Magnussen, S. Wu and J. Lipkowski. *J. Electroanal. Chem.* 409 (1996), p. 155.
- [106] J. Wang, B.M. Ocko, A.J. Davenport and H.S. Isaacs. *Phys. Rev. B* 46 (1992), p. 10321.
- [107] S.W.u Lipkowski, J. Magnussen, O.M. Ocko and B.M. Th. Wandlowski. *J. Electroanal. Chem.* 446 (1998), p. 67.

9. SUMMARY IN ESTONIAN

Kompaktseid adsorbseid kilesid moodustavate orgaaniliste ühendite adsorptsiooni termodünaamika ja kineetika vismuti monokristalli tahkudel

Käesolevas töös uuriti vismuti monokristalli tahkudel uratsiili, tetrabutüülammoonium katiooni (TBA^+), naatriumdodetsüülsulfaadi (SDS), kampri ja 2, 2'-bipüridiini (2, 2'BP) adsorptsiooni kineetikat ja termodünaamilisi parameetreid impedantspektroskoopia ja *in situ* STM meetodiga.

Vahelduvvoolu sagedusspektreid analüüsiti erinevate ekvivalentsskeemide abil nagu Frumkin-Melik-Gaikazian, modifitseeritud Frumkin-Melik-Gaikazian, Wandlowski-de Levie jne.

Eksperimentaalsete sagedusspektrite mittelineaarsel regressioonanalüüsil leiti, et uuritavate süsteemide vähemkontsentreeritud lahustes on adsorptsioon esimeses lähenduses kirjeldatav klassikalise Frumkin-Melik-Gaikaziani adsorptsiooni kineetika mudeliga. Kontsentreeritumate lahuste puhul tuleb rakendada oluliselt keerukamaid adsorptsioonimudeleid, mis kirjeldavad adsorbse kihis toimuvaid reorganisatsiooni, reorientatsiooni ja ka kahedimensionaalse kile moodustumise protsesse. Seega leiti, et maksimaalse adsorptsiooni alas kontsentreeritumate adsorbaadi lahuste puhul kirjeldab uuritavat süsteemi kõige paremini Wandlowski de Levie mudel, mis võtab arvesse ka kompaktse adsorptsioonilise kihi teket. Adsorptsioonimudeli alusel leitud mahtuvused: C_{true} , C_{ad} , ja C_n on minimaalsed ja takistused: R_N ja R_D maksimaalsed maksimaalse adsorptsiooni alas. See näitab kompaktse adsorbse kihi moodustumist $Bi(hkl)$ pinnal $E = E_{max}$ potentsiaalil. Mahtuvused kasvavad ja takistused vähenevad kiiresti negatiivse pinnalaengu kasvades.

Kompleksjuhtivuse paralleelmahtuvusest sõltuvuste, so Cole-Cole sõltuvustest, leiti, et maksimaalse adsorptsiooni alas on kampri adsorptsioon elektroodi pinnale limiteeritud heterogeense adsorptsiooni staadiumi poolt. 2, 2'-BP, SDS, TBA^+ ja uratsiili adsorptsiooni elektroodi pinnale kirjeldab segakineetika mudel, mis arvestab aeglast difusiooni- ja adsorptsioonistaadiumit. Võrreldes teiste uuritavate süsteemidega on TBA^+ adsorptsiooni korral kõrvalekalle difusioonilimiteeritud kineetilisest käitumisest tühine. Määratud eksperimentaalsed adsorptsiooniprotsessi relaksatsioonikonstandid sõltuvad märkimisväärselt elektroodi potentsiaalst, adsorbaadi kontsentratsioonist, adsorbaadi keemilisest loomusest ja elektroodi pinna krsitallograafilisest loomusest. Arvutatud teoreetilised relaksatsiooniajad olid kooskõlas eksperimentaalsetega.

Käsitletud süsteemidele konstrueeritud Frumkini adsorptsiooniisotermid on lineaarsed vahemikus $0.1 < \theta < 0.8$. Frumkini adsorptsiooniisotermi tõusudest leitud molekulide vahelise interaktsiooni iseloomustava parameetri a positiivsed väärtused ja Gibbsi interaktsioonienergia negatiivsed väärtused näitavad, et

adsorbaat-adsorbaat ja vesi-vesi interaktsioonid on tugevamad, kui adsorbaat-vesi vahelised interaktsioonid.

Adsorbeerunud aine ruumala S_{\max} väheneb ja Gibbsi adsorptsioon Γ_{\max} kasvab järjekorras $\text{TBA}^+ < \text{SDS} < \text{uratsiil} < \text{kamper} < \text{2,2'-BP}$, mis on seletatav kompaktsema kile moodustumisega adsorbtses kihis.

Gibbsi adsorptsiooni vabaenergia $-\Delta G_A^0$ kasvab reas: $\text{uratsiil} < \text{kamper} < \text{SDS} < \text{2,2'-BP}$, mis vastab adsorptsioonilise aktiivsuse kasvule eelpool toodud reas.

10. ACKNOWLEDGEMENTS

The present study was performed at the Institute of Physical Chemistry of the University of Tartu. The support was received from Estonian Science Foundation (grants 5803, 6696 and 6970) and Doctoral School of Material Science and Material Technology.

First and foremost I would like to express my gratitude to my supervisor Professor Enn Lust for persistent assistance and scientific guidance through the years of our collaboration.

I am very thankful to my supervisor Gunnar Nurk, who has always found time for scientific discussions and were there when I needed help with different technical problems.

I would like to thank all my friends and colleagues for helpful discussions, inspirations and continuous support.

My warmest thanks go to my parents for their patients and understanding over the years.

11. PUBLICATIONS

CURRICULUM VITAE

General data

1. *First Name and surname:* Heili Kasuk
2. *Date and place of birth:* 4.08.1980, Jõgeva
3. *Citizenship:* Estonian
4. *Marital status:* unmarried
5. *Address:* Pärna 21a–17, 50604 Tartu
Telephone number: 55 540 751
e-mail address: heili.kasuk@ut.ee
6. *Present employment:* University of Tartu, Institute of Physical Chemistry, researcher (0.1)
University of Tartu, Doctoral School of Material Science and Material Technology, researcher (0.1)

Education

- 2003– ... University of Tartu, Ph.D. student (physical and electrochemistry)
2003– University of Tartu, M. Sc. in physical and electrochemistry
2002– University of Tartu, B. Sc. in chemistry
1998– Nõo Secondary Science School

Professional employment and retraining

- 2007– ... University of Tartu, Institute of Physical Chemistry, temporary researcher (0.1)
5.09.2005–17.08.2007 University of Tartu, Institute of Physical Chemistry, secretary (0.8)
01.10.2005–31.08.2007 University of Tartu, Doctoral School of Material Science and Material Technology, researcher (0.1).
01.10.2003–31.12.2003 The Royal Institut of Technology (KTH), Stockholm, guest researcher.
2001–2005 University of Tartu, Institute of Physical Chemistry, laboratorian.

Major scientific publications

1. **H. Kasuk**, G. Nurk, K. Lust and E. Lust, Adsorption kinetics of uracil on the bismuth single crystal planes, *J. Electroanal. Chem.* 550–551 (2003) 13–31.
2. G. Nurk, **H. Kasuk**, K. Lust, A. Jänes and E. Lust, Adsorption kinetics of dodecyl sulfate anions on the bismuth (01 $\bar{1}$) plane, *J. Electroanal. Chem.* 553 (2003) 1–19.
3. K. Laes, **H. Kasuk**, G. Nurk, M. Väärtnõu, K. Lust, A. Jänes and E. Lust, Adsorption kinetics of tetrabutylammonium cations on Bi(01 $\bar{1}$) plane, *J. of Electroanal. Chem.*, 569 (2004) 241–256.
4. **H. Kasuk**, G. Nurk, K. Lust and E. Lust, Adsorption of uracil on bismuth single crystal planes, *J. Electroanal. Chem.*, 580 (2005) 128–134.
5. S. Kallip, **H. Kasuk**, V. Grozovski, P. Möller, E. Lust, Adsorption of camphor and 2, 2'-bipyridin on Bi(111) electrode surface, *ECS Transactions*, 3 (2007), accepted.
6. S. Kallip, **H. Kasuk**, V. Grozovski, P. Möller, E. Lust, Adsorption kinetics of camphor and 2, 2'-bipyridin on Bi(111) electrode surface, *Electrochim. Acta*, in review.
7. **H. Kasuk**, G. Nurk, E. Lust, Adsorption of dodecyl sulfate anion on the Bi(111), Bi(001) and Bi(01 $\bar{1}$) planes, *J. Electroanal. Chem.*, in press.
8. **H. Kasuk**, M. Veelma, G. Nurk, E. Lust, Adsorption kinetics of Na₂EDTA at bismuth single crystal planes, in prep.

CURRICULUM VITAE

1. *Ees- ja perekonnanimi:* Heili Kasuk
2. *Sünniaeg ja koht:* 4.08.1980, Jõgevamaa
3. *Kodakondsus:* Eesti
4. *Perekonnaseis:* vallaline
5. *Aadress:* Pärna 21A–17, 50604 Tartu
Telefoni number: 55 540 751
e-maili aadress: heili.kasuk@ut.ee
6. *Praegune töökoht:* Tartu Ülikool, Füüsikalise keemia instituut, füüsikalise ja elektrokeemia erakorraline teadur (0.1 koormust),
Tartu Ülikool, Materjaliteaduse ja materjalide tehnoloogia doktorikool, erakorraline teadur (0.1 koormust).

Haridus

- 2003 – ... Tartu Ülikool, füüsika-keemiateaduskond, doktorant füüsikalise ja elektrokeemia erialal
- 2003 – Tartu Ülikool, füüsika-keemiateaduskond, M. Sc füüsikalise ja elektrokeemia erialal
- 2002 – Tartu Ülikool, füüsika-keemiateaduskond, B. Sc kraad keemias
- 1998 – Nõo Reaalgümnaasium

Teenistuskäik

- 2007 – ... Tartu Ülikool, Füüsikalise keemia instituut, füüsikalise ja elektrokeemia erakorraline teadur (0.1 koormust)
- 5.09.2005–17.08.2007 Tartu Ülikool, Füüsikalise keemia instituut, vastutav sekretär (0.8 koormust)
- 01.10.2005–31.08.2007 Tartu Ülikool, Materjaliteaduse ja materjalide tehnoloogia doktorikool, erakorraline teadur (0.1 koormust).
- 01.10.2003–31.12.2003 Stockholmi Kuninglik Tehnoloogiainstituut, külalisteadur
- 2001 – 2005 Tartu Ülikool, Füüsikalise keemia instituut, laborant.

Olulisemad publikatsioonid

1. **H. Kasuk**, G. Nurk, K. Lust and E. Lust, Adsorption kinetics of uracil on the bismuth single crystal planes, *J. Electroanal. Chem.* 550–551 (2003) 13–31.
2. G. Nurk, **H. Kasuk**, K. Lust, A. Jänes and E. Lust, Adsorption kinetics of dodecyl sulfate anions on the bismuth (01 $\bar{1}$) plane, *J. Electroanal. Chem.* 553 (2003) 1–19.
3. K. Laes, **H. Kasuk**, G. Nurk, M. Väärtnõu, K. Lust, A. Jänes and E. Lust, Adsorption kinetics of tetrabutylammonium cations on Bi(01 $\bar{1}$) plane, *J. of Electroanal. Chem.*, 569 (2004) 241–256.
4. **H. Kasuk**, G. Nurk, K. Lust and E. Lust, Adsorption of uracil on bismuth single crystal planes, *J. Electroanal. Chem.*, 580 (2005) 128–134.
5. S. Kallip, **H. Kasuk**, V. Grozovski, P. Möller, E. Lust, Adsorption of camphor and 2, 2'-bipyridin on Bi(111) electrode surface, *ECS Transactions*, 3 (2007), accepted.
6. S. Kallip, **H. Kasuk**, V. Grozovski, P. Möller, E. Lust, Adsorption kinetics of camphor and 2, 2'-bipyridin on Bi(111) electrode surface, *Electrochim. Acta*, in review.
7. **H. Kasuk**, G. Nurk, E. Lust, Adsorption of dodecyl sulfate anion on the Bi(111), Bi(001) and Bi(01 $\bar{1}$) planes, *J. Electroanal. Chem.*, in press.
8. **H. Kasuk**, M. Veelma, G. Nurk, E. Lust, Adsorption kinetics of Na₂EDTA at bismuth single crystal planes, in prep.

DISSERTATIONES CHIMICAE UNIVERSITATIS TARTUENSIS

1. **Toomas Tamm.** Quantum-chemical simulation of solvent effects. Tartu, 1993, 110 p.
2. **Peeter Burk.** Theoretical study of gas-phase acid-base equilibria. Tartu, 1994, 96 p.
3. **Victor Lobanov.** Quantitative structure-property relationships in large descriptor spaces. Tartu, 1995, 135 p.
4. **Vahur Mäemets.** The ^{17}O and ^1H nuclear magnetic resonance study of H_2O in individual solvents and its charged clusters in aqueous solutions of electrolytes. Tartu, 1997, 140 p.
5. **Andrus Metsala.** Microcanonical rate constant in nonequilibrium distribution of vibrational energy and in restricted intramolecular vibrational energy redistribution on the basis of Slater's theory of unimolecular reactions. Tartu, 1997, 150 p.
6. **Uko Maran.** Quantum-mechanical study of potential energy surfaces in different environments. Tartu, 1997, 137 p.
7. **Alar Jänes.** Adsorption of organic compounds on antimony, bismuth and cadmium electrodes. Tartu, 1998, 219 p.
8. **Kaido Tammeveski.** Oxygen electroreduction on thin platinum films and the electrochemical detection of superoxide anion. Tartu, 1998, 139 p.
9. **Ivo Leito.** Studies of Brønsted acid-base equilibria in water and non-aqueous media. Tartu, 1998, 101 p.
10. **Jaan Leis.** Conformational dynamics and equilibria in amides. Tartu, 1998, 131 p.
11. **Toonika Rinken.** The modelling of amperometric biosensors based on oxidoreductases. Tartu, 2000, 108 p.
12. **Dmitri Panov.** Partially solvated Grignard reagents. Tartu, 2000, 64 p.
13. **Kaja Orupõld.** Treatment and analysis of phenolic wastewater with microorganisms. Tartu, 2000, 123 p.
14. **Jüri Ivask.** Ion Chromatographic determination of major anions and cations in polar ice core. Tartu, 2000, 85 p.
15. **Lauri Vares.** Stereoselective Synthesis of Tetrahydrofuran and Tetrahydropyran Derivatives by Use of Asymmetric Horner-Wadsworth-Emmons and Ring Closure Reactions. Tartu, 2000, 184 p.
16. **Martin Lepiku.** Kinetic aspects of dopamine D_2 receptor interactions with specific ligands. Tartu, 2000, 81 p.
17. **Katrin Sak.** Some aspects of ligand specificity of P2Y receptors. Tartu, 2000, 106 p.
18. **Vello Pällin.** The role of solvation in the formation of iotsitch complexes. Tartu, 2001, 95 p.

19. **Katrin Kollist.** Interactions between polycyclic aromatic compounds and humic substances. Tartu, 2001, 93 p.
20. **Ivar Koppel.** Quantum chemical study of acidity of strong and superstrong Brønsted acids. Tartu, 2001, 104 p.
21. **Viljar Pihl.** The study of the substituent and solvent effects on the acidity of OH and CH acids. Tartu, 2001, 132 p.
22. **Natalia Palm.** Specification of the minimum, sufficient and significant set of descriptors for general description of solvent effects. Tartu, 2001, 134 p.
23. **Sulev Sild.** QSPR/QSAR approaches for complex molecular systems. Tartu, 2001, 134 p.
24. **Ruslan Petrukhin.** Industrial applications of the quantitative structure-property relationships. Tartu, 2001, 162 p.
25. **Boris V. Rogovoy.** Synthesis of (benzotriazolyl)carboximidamides and their application in relations with *N*- and *S*-nucleophiles. Tartu, 2002, 84 p.
26. **Koit Herodes.** Solvent effects on UV-vis absorption spectra of some solvatochromic substances in binary solvent mixtures: the preferential solvation model. Tartu, 2002, 102 p.
27. **Anti Perkson.** Synthesis and characterisation of nanostructured carbon. Tartu, 2002, 152 p.
28. **Ivari Kaljurand.** Self-consistent acidity scales of neutral and cationic Brønsted acids in acetonitrile and tetrahydrofuran. Tartu, 2003, 108 p.
29. **Karmen Lust.** Adsorption of anions on bismuth single crystal electrodes. Tartu, 2003, 128 p.
30. **Mare Piirsalu.** Substituent, temperature and solvent effects on the alkaline hydrolysis of substituted phenyl and alkyl esters of benzoic acid. Tartu, 2003, 156 p.
31. **Meeri Sassian.** Reactions of partially solvated Grignard reagents. Tartu, 2003, 78 p.
32. **Tarmo Tamm.** Quantum chemical modelling of polypyrrole. Tartu, 2003. 100 p.
33. **Erik Teinmaa.** The environmental fate of the particulate matter and organic pollutants from an oil shale power plant. Tartu, 2003. 102 p.
34. **Jaana Tammiku-Taul.** Quantum chemical study of the properties of Grignard reagents. Tartu, 2003. 120 p.
35. **Andre Lomaka.** Biomedical applications of predictive computational chemistry. Tartu, 2003. 132 p.
36. **Kostyantyn Kirichenko.** Benzotriazole — Mediated Carbon–Carbon Bond Formation. Tartu, 2003. 132 p.
37. **Gunnar Nurk.** Adsorption kinetics of some organic compounds on bismuth single crystal electrodes. Tartu, 2003, 170 p.
38. **Mati Arulepp.** Electrochemical characteristics of porous carbon materials and electrical double layer capacitors. Tartu, 2003, 196 p.

39. **Dan Cornel Fara.** QSPR modeling of complexation and distribution of organic compounds. Tartu, 2004, 126 p.
40. **Riina Mahlapuu.** Signalling of galanin and amyloid precursor protein through adenylate cyclase. Tartu, 2004, 124 p.
41. **Mihkel Kerikmäe.** Some luminescent materials for dosimetric applications and physical research. Tartu, 2004, 143 p.
42. **Jaanus Kruusma.** Determination of some important trace metal ions in human blood. Tartu, 2004, 115 p.
43. **Urmas Johanson.** Investigations of the electrochemical properties of polypyrrole modified electrodes. Tartu, 2004, 91 p.
44. **Kaido Sillar.** Computational study of the acid sites in zeolite ZSM-5. Tartu, 2004, 80 p.
45. **Aldo Oras.** Kinetic aspects of dATP α S interaction with P2Y₁ receptor. Tartu, 2004, 75 p.
46. **Erik Mölder.** Measurement of the oxygen mass transfer through the air-water interface. Tartu, 2005, 73 p.
47. **Thomas Thomberg.** The kinetics of electroreduction of peroxodisulfate anion on cadmium (0001) single crystal electrode. Tartu, 2005, 95 p.
48. **Olavi Loog.** Aspects of condensations of carbonyl compounds and their imine analogues. Tartu, 2005, 83 p.
49. **Siim Salmar.** Effect of ultrasound on ester hydrolysis in aqueous ethanol. Tartu, 2006, 73 p.
50. **Ain Uustare.** Modulation of signal transduction of heptahelical receptors by other receptors and G proteins. Tartu, 2006, 121 p.
51. **Sergei Yurchenko.** Determination of some carcinogenic contaminants in food. Tartu, 2006, 143 p.
52. **Kaido Tämm.** QSPR modeling of some properties of organic compounds. Tartu, 2006, 67 p.
53. **Olga Tšubrik.** New methods in the synthesis of multisubstituted hydrazines. Tartu, 2006, 183 p.
54. **Lilli Sooväli.** Spectrophotometric measurements and their uncertainty in chemical analysis and dissociation constant measurements. Tartu, 2006, 125 p.
55. **Eve Koort.** Uncertainty estimation of potentiometrically measured pH and pK_a values. Tartu, 2006, 139 p.
56. **Sergei Kopanchuk.** Regulation of ligand binding to melanocortin receptor subtypes. Tartu, 2006, 119 p.
57. **Silvar Kallip.** Surface structure of some bismuth and antimony single crystal electrodes. Tartu, 2006, 107 p.
58. **Kristjan Saal.** Surface silanization and its application in biomolecule coupling. Tartu, 2006, 77 p.
59. **Tanel Tätte.** High viscosity Sn(OBu)₄ oligomeric concentrates and their applications in technology. Tartu, 2006, 91 p.

60. **Dimitar Atanasov Dobchev**. Robust QSAR methods for the prediction of properties from molecular structure. Tartu, 2006, 118 p.
61. **Hannes Hagu**. Impact of ultrasound on hydrophobic interactions in solutions. Tartu, 2007, 81 p.
62. **Rutha Jäger**. Electroreduction of peroxodisulfate anion on bismuth electrodes. Tartu, 2007, 142 p.
63. **Kaido Viht**. Immobilizable bisubstrate-analogue inhibitors of basophilic protein kinases: development and application in biosensors. Tartu, 2007, 88 p.
64. **Eva-Ingrid Rõõm**. Acid-base equilibria in nonpolar media. Tartu, 2007, 156 p.
65. **Sven Tamp**. DFT study of the cesium cation containing complexes relevant to the cesium cation binding by the humic acids. Tartu, 2007, 102 p.
66. **Jaak Nerut**. Electroreduction of hexacyanoferrate(III) anion on Cadmium (0001) single crystal electrode. Tartu, 2007, 180 p.
67. **Lauri Jalukse**. Measurement uncertainty estimation in amperometric dissolved oxygen concentration measurement. Tartu, 2007, 112 p.
68. **Aime Lust**. Charge state of dopants and ordered clusters formation in CaF₂:Mn and CaF₂:Eu luminophors. Tartu, 2007, 100 p.
69. **Iiris Kahn**. Quantitative Structure-Activity Relationships of environmentally relevant properties. Tartu, 2007, 98 p.
70. **Mari Reinik**. Nitrates, nitrites, N-nitrosamines and polycyclic aromatic hydrocarbons in food: analytical methods, occurrence and dietary intake. Tartu, 2007, 172 p.